The Plant Cell, Vol. 30: 117–133, January 2018, www.plantcell.org © 2018 ASPB.

PWWP-DOMAIN INTERACTOR OF POLYCOMBS1 Interacts with Polycomb-Group Proteins and Histones and Regulates Arabidopsis Flowering and Development

Mareike L. Hohenstatt,[a,1] Pawel Mikulski,[a,b,1,2] Olga Komarynets,[a,c] Constanze Klose,[a] Ina Kycia,[d,3] Albert Jeltsch,[d] Sara Farrona,[a,e,4,5] and Daniel Schubert[a,b,4,5]

[a] Institute for Genetics, Heinrich-Heine-University, 40225 Duesseldorf, Germany
[b] Institute of Biology, Freie Universität, 14195 Berlin, Germany
[c] Université de Genève, 1205 Geneva, Switzerland
[d] Institute for Biochemistry, University of Stuttgart, 70174 Stuttgart, Germany
[e] Plant and AgriBiosciences Centre, National University Ireland, Galway H91 TK33, Ireland

ORCID IDs: 0000-0001-6113-9290 (A.J.); 0000-0003-2390-0733 (D.S.)

Polycomb-group (PcG) proteins mediate epigenetic gene regulation by setting H3K27me3 via Polycomb Repressive Complex 2 (PRC2). In plants, it is largely unclear how PcG proteins are recruited to their target genes. Here, we identified the PWWP-DOMAIN INTERACTOR OF POLYCOMBS1 (PWO1) protein, which interacts with all three *Arabidopsis thaliana* PRC2 histone methyltransferases and is required for maintaining full H3 occupancy at several Arabidopsis genes. PWO1 localizes and recruits CURLY LEAF to nuclear speckles in *Nicotiana benthamiana* nuclei, suggesting a role in spatial organization of PcG regulation. *PWO1* belongs to a gene family with three members having overlapping activities: *pwo1 pwo2 pwo3* triple mutants are seedling lethal and show shoot and root meristem arrest, while *pwo1* single mutants are early flowering. Interestingly, the PWWP domain of PWO1 confers binding to histones, which is reduced by a point mutation in a highly conserved residue of this domain and blocked by phosphorylation of H3S28. PWO1 carrying this mutation is not able to fully complement the *pwo1 pwo2 pwo3* triple mutant, indicating the requirement of this domain for PWO1 in vivo activity. Thus, the PWO family may present a novel class of histone readers that are involved in recruiting PcG proteins to subnuclear domains and in promoting Arabidopsis development.

INTRODUCTION

Polycomb group (PcG) and the antagonistically acting Trithorax group (TrxG) proteins are key regulators of epigenetic gene regulation which are essential for the development of eukaryotic organisms (Kondo et al., 2016; Mozgova and Hennig, 2015). Initially identified in *Drosophila melanogaster*, PcG proteins maintain repression of homeotic gene expression, while the TrxG proteins sustain activation of homeotic genes through cell division, thus conferring epigenetic memory.

PcG proteins act in several high molecular weight complexes, the so-called Polycomb repressive complexes (PRC) (Mozgova and Hennig, 2015; Schuettengruber et al., 2007; Simon and Kingston, 2013). PRC2 consists of four core members in Drosophila, Enhancer of zeste [E(z)], Extra sex combs (Esc), p55, and Suppressor of zeste12 [Su(z)12]. The PRC2 complex mediates trimethylation of H3K27 through the SET domain of its subunit E(z) (Cao et al., 2002; Cao and Zhang, 2004; Czermin et al., 2002; Kuzmichev et al., 2002; Müller et al., 2002). Although the H3K27me3 mark is required for gene repression, the presence of this mark does not always correlate with the transcriptional status of the gene where it is present, indicating a more complex regulation and the involvement of other factors (Bouyer et al., 2011; Farrona et al., 2011; Lafos et al., 2011). An additional complex, PRC1, has also been related to this activity. The PRC1 subunit Polycomb (Pc) specifically binds to H3K27me3 via its chromodomain. Thus, in the classical PcG model, PRC1 recognizes the presence of this histone mark and then inhibits nucleosome remodeling and transcription, compacts chromatin, and ubiquitinates histone H2A (de Napoles et al., 2004; Fischle et al., 2003; Francis et al., 2001, 2004; Shao et al., 1999; Wang et al., 2004). However, more recent data indicate that the hierarchical recruitment of PRCs may be far more complex. Indeed, studies in plants and animals showed that PRC1 activity is required for proper H3K27me3 deposition to specific targets and PRC1 components have been found directly interacting with PRC2 components (Del Prete et al., 2015; Merini and Calonje, 2015; Schwartz and Pirrotta, 2014). In addition, it has recently been shown that PRC1-mediated repression can also occur in the absence of H2A monoubiquitination, indicating different PcG silencing scenarios (Calonje, 2014; Illingworth et al., 2015; Pengelly et al., 2015).

[1] These authors contributed equally to this work.
[2] Current address: John Innes Centre, Norwich NR4 7UH, UK.
[3] Current address: The Jackson Laboratory for Genomic Medicine, Farmington, CT 06032.
[4] These authors contributed equally to this work.
[5] Address correspondence to sara.farrona@nuigalway.ie or dan.schubert@fu-berlin.de.
The authors responsible for distribution of materials integral to the findings presented in this article in accordance with the policy described in the Instructions for Authors (www.plantcell.org) are: Sara Farrona (sara.farrona@nuigalway.ie) and Daniel Schubert (dan.schubert@fu-berlin.de).
www.plantcell.org/cgi/doi/10.1105/tpc.17.00117

Recruitment of PcG proteins to the chromatin may occur by several mechanisms, including binding of H3K36me3 by the PRC2-associated protein Polycomb-like, binding to transcription factors and to CpG dinucleotides in CpG islands, interaction of PhoRC with specific DNA sequences, the Polycomb response elements (PREs), and direct binding of long noncoding RNAs by PRC2 (Cai et al., 2013; Del Prete et al., 2015; Deng et al., 2013; Klose et al., 2013; Schuettengruber and Cavalli, 2009; Simon and Kingston, 2013). PRE-like sequences have recently been identified at thousands of loci in plants, and the presence of specific *cis*-regulatory elements (e.g., GAGA motives, telo boxes) in these sequences has been related to PcG recruitment (Berger et al., 2011; Deng et al., 2013; Hecker et al., 2015; Lodha et al., 2013; Wang et al., 2016; Xiao et al., 2017; Zhou et al., 2016). Binding of PRC2 and PRC1 components to long noncoding RNAs has also been shown in plants (Ariel et al., 2014; Heo and Sung, 2011). Nevertheless, while there is now good evidence for PRE-like sequences in plants, it remains elusive whether these elements are generally sufficient for PRC2 recruitment at the thousands of PcG target genes in *Arabidopsis thaliana*.

All four subunits of the Drosophila PRC2 complex are conserved in Arabidopsis. Except for the single-copy gene *FERTILIZATION INDEPENDENT ENDOSPERM*, which is the ortholog of Esc, all subunits are encoded by small gene families (Mozgova and Hennig, 2015; Ohad et al., 1999). The catalytic subunit E(z) is represented by three genes in the Arabidopsis genome encoded by *CURLY LEAF* (*CLF*), *SWINGER* (*SWN*), and *MEDEA* (*MEA*) (Goodrich et al., 1997; Grossniklaus et al., 1998; Luo et al., 1999). In addition, Su(z)12 is orthologous to the Arabidopsis genes *VERNALIZATION2* (*VRN2*), *EMBRYONIC FLOWER2* (*EMF2*), and *FERTILIZATION INDEPENDENT SEED2* (*FIS2*) (Gendall et al., 2001; Luo et al., 1999; Yoshida et al., 2001). The genes *MULTICOPY SUPPRESSOR OF IRA1-5* (*MSI1-5*) have sequence homology to the WD40 protein p55, and MSI1 and MSI4 were found to be associated with the Arabidopsis PRC2 complex (Derkacheva et al., 2013; Köhler et al., 2003; Pazhouhandeh et al., 2011). Genetic studies suggest the existence of at least three PRC2 complexes in Arabidopsis: the VRN-PRC2 complex, which is involved in the vernalization response; the FIS-PRC2 complex required to inhibit fertilization-independent seed development; and the EMF-PRC2 complex, which is needed for the suppression of precocious, embryonic flowering and for floral organ development (Förderer et al., 2016; Mozgova and Hennig, 2015). Hence, the different complexes control important transitions at different stages of plant development and are therefore crucial for completion of the life cycle (Butenko and Ohad, 2011; Förderer et al., 2016; Mozgova et al., 2015). Genome-wide profiling of PRC2 target genes has revealed the existence of more than 8000 genes carrying the H3K27me3 mark in Arabidopsis (Bouyer et al., 2011; Lafos et al., 2011; Oh et al., 2008; Roudier et al., 2011; Zhang et al., 2007). These studies identified previously known target genes of the three potential PRC2 complexes, but also identified targets involved in stress responses, hormonal signal transduction pathways, promotion of embryonic growth, and microRNA genes, suggesting that additional PRC2 complexes may exist.

It is likely that plant-specific components of PRCs have evolved to fulfill a similar function to the nonconserved Drosophila PcG proteins or have functions specific to plant growth and development. Recently, several PRC2 components have been identified that modulate PRC2 activity: VRN5 and VIN3 associate with PRC2 to form a PHD-PRC2 to achieve high levels of H3K27me3, similar to Drosophila Pcl-PRC2 and human hPHF1-PRC2 (Greb et al., 2007; Nekrasov et al., 2007; Cao et al., 2008; Sarma et al., 2008). Additional PcG-associated proteins encoded only in plant genomes have been either identified in genetic screens for suppressors of *lhp1* and *clf* (ANTAGONISTIC OF LHP1 [ALP1], TELOMERE REPEAT BINDING, and an Arabidopsis *Chromosome transmission fidelity4* homolog) and by protein-protein interaction screens (BLISTER and ALFIN1-like proteins) (Liang et al., 2015; Molitor et al., 2014; Schatlowski et al., 2010; Sung and Amasino, 2004; Zhou et al., 2016, 2017). Although ALP1 is found in PRC2 complexes, it antagonizes PRC2 function, suggesting that PRC2 activity can be modulated at various levels. How the other PRC2-associated proteins molecularly contribute to PcG silencing is largely unresolved.

Thus, PcG target genes are regulated at multiple levels, including recruitment of PcG proteins, a combination of multiple repressive modifications, absence of activating modifications, and binding/interpretation of the marks. While the role of PRC2 and PRC1-like proteins in plant development is relatively well understood, many regulators controlling additional molecular functions in PcG silencing are awaiting discovery.

In this study, we identified the novel, plant-specific PWWP-domain protein PWWP-DOMAIN INTERACTOR OF POLYCOMBS (PWO1), which interacts with all three PRC2 histone methyltransferase subunits from Arabidopsis. PWO1 localizes to euchromatic regions in *Nicotiana benthamiana* nuclei, both in the nucleoplasm and in nuclear speckles. PWO1 contributes to PcG silencing by repressing a subset of PcG targets. While H3K27me3 levels are reduced at these loci in *pwo1* mutants, this is largely explained by a reduction in H3 occupancy, suggesting that PWO1 contributes to chromatin compaction. *pwo1* mutants are early flowering due to reduced levels of the floral repressor *FLOWERING LOCUS C* (*FLC*). We show that PWO1 has a much broader role in development as it has overlapping functions with two homologous proteins to maintain shoot and root meristems. Interestingly, the putative chromatin reading PWWP domain of PWO1 is required for nuclear speckle formation and confers binding to histone 3 (H3) in vitro. This function is inhibited by phosphorylation of H3S28, a mark counteracting PcG silencing. A point mutation of PWO1's PWWP domain strongly reduces PWO1-H3 interaction in vitro and, when transformed in the *pwo1 pwo2 pwo3* background, is unable to fully complement the triple mutant inducing developmental abnormalities at the shoot apical meristem. Thus, we identify the PWO family as essential regulators of Arabidopsis development that recruit PRC2 to specific regions on the chromatin by interacting with H3 through its PWWP domain.

RESULTS

Identification of PWO1 as an Interactor of PcG Proteins

To discover proteins involved in PcG-mediated gene silencing, we performed a yeast two-hybrid screen with a truncated CLF protein as bait (Schatlowski et al., 2010). This screen yielded the Su(z)12 homologs EMF2 and VRN2 and the PcG-associated protein BLISTER (Schatlowski et al., 2010). We revisited the list of potential CLF

interaction partners to identify proteins containing putative chromatin "reading" domains. This analysis identified the protein At3g03140, which contains 769 amino acids and comprises a predicted N-terminal PWWP domain as well as a central nuclear localization signal (NLS) (Figure 1B). PWWP domains belong to the "royal family," which includes the Tudor, Chromatin binding (Chromo), Malignant Brain Tumor (MBT), PWWP, and Agenet domains and is implicated in methyl-lysine/arginine binding (Maurer-Stroh et al., 2003). Subsequently, we confirmed the interaction with CLF in independent yeast two-hybrid analyses and further revealed a potential interaction with the two homologs of CLF, SWN and MEA, and homodimerization of At3g03140 (Figure 1A). We therefore named At3g03140 PWWP-DOMAIN INTERACTOR OF POLYCOMBS1 (PWO1). To confirm the interaction in vivo, we generated *PWO1*$_{pro}$*:PWO1-GFP i35S*$_{pro}$*:mCHERRY-CLF* double transgenic Arabidopsis lines. The *i35S*$_{pro}$*:mCHERRY-CLF* line allows estradiol-dependent induction of mCHERRY-CLF and, therefore, controlled expression levels. After estradiol induction, proteins were isolated and subjected to coimmunoprecipitation analyses. Anti-GFP antibodies precipitated PWO1-GFP and also pulled down mCHERRY-CLF, suggesting that PWO1 and CLF are part of the same complex in planta (Figure 1C).

While PWWP-domain proteins are found in most eukaryotic organisms, proteins with high similarity to PWO1 are only found in plants, including two close Arabidopsis homologs that we named *PWO2* and *PWO3* (Supplemental Figure 1). An alignment of the protein sequences of PWO1/2/3 shows the highest similarity in the N-terminal region of the proteins containing the predicted PWWP domain and in the C-terminal region (Supplemental Figure 1).

PWO1 Is Widely Expressed and Tethers CLF to Nuclear Speckles in Tobacco

To analyze the expression pattern of *PWO1*, a translational fusion of the PWO1 genomic locus to a C-terminal uidA reporter gene (*PWO1*$_{pro}$*:PWO1-GUS*) was constructed and introduced into Columbia-0 (Col-0) plants by *Agrobacterium tumefaciens*-mediated transformation. Analysis of homozygous *PWO1*$_{pro}$*:PWO1-GUS* reporter lines revealed *PWO1* expression in the vasculature of the root and shoot, cotyledons, and rosette leaves of young seedlings. In addition, expression was observed in the primary root tip as well as in developing side roots. In flowers, expression of the fusion protein was detectable in sepals and carpels (Figure 2B). Thus, *PWO1* expression is widely expressed, preferentially in less differentiated tissues, and broadly overlaps with that of the PcG genes *CLF* and *SWN* (Chanvivattana et al., 2004; Goodrich et al., 1997).

As PcG proteins are localized to euchromatic regions of the nucleus, we asked whether PWO1 shows similar localization. We therefore analyzed PWO1 localization in a *PWO1*$_{pro}$*:PWO1-GFP* Arabidopsis line. Consistent with the predicted NLS, the PWO1-GFP fusion protein showed nuclear localization in Arabidopsis root cells (Figure 2A). In addition, immunofluorescence analyses on isolated nuclei of the *PWO1*$_{pro}$*:PWO1-GFP* line revealed a nonuniform nuclear distribution of PWO1 and uncovered an exclusion from the heterochromatic chromocenters, which are densely stained by the DNA stain DAPI (4′,6-diamidino-2-phenylindole), suggesting that PWO1 is a euchromatic protein (Figure 2C).

To assess whether PWO1 colocalizes with its interaction partner CLF, PWO1-mCherry (*i35S*$_{pro}$*:PWO1-mCherry*) was transiently coexpressed with GFP-CLF (*i35S*$_{pro}$*:GFP-CLF*) in *N. benthamiana.* Both fusion proteins localized to the nucleus, which is consistent with the interaction of PWO1 with CLF (Figures 2D to 2I). Interestingly, PWO1-mCherry showed localization not only to the nucleoplasm, but also to a variable amount of nuclear speckles of unknown identity. GFP-CLF localized either uniformly or in larger patches to the nucleus but never to speckles when expressed alone. However, when PWO1-mCherry was coexpressed with GFP-CLF, one-third of nuclei (5 of 15 nuclei) showed speckle formation for GFP-CLF, which largely overlap with the PWO1 speckles. In addition, another third of nuclei (5 of 15 nuclei) displayed localization of both PWO1 and CLF to larger patches in the nucleus, which was not observed in PWO1-mCherry single transformations. Analyses of the confocal images demonstrated an increase in speckle intensity when both proteins were cotransformed together (Figure 2J). Hence, subnuclear localization of both PWO1 and CLF in a heterologous system depends on each other and provides further evidence that they may form a complex in vivo.

Role of the PWO Family in Flowering Time and Seedling Development

To analyze PWO1 function during Arabidopsis development, two independent lines with a T-DNA insertion in the *PWO1* gene and a line carrying a premature stop codon in the PWWP domain were isolated and homozygous plants were analyzed. As the stop codon results in a truncated protein of only 45 amino acids, this allele likely reflects a loss-of-function allele (Supplemental Figure 2). All three *pwo1* alleles had no obvious leaf or flower defects; however, they consistently showed a moderate early flowering phenotype in long-day (LD) and short-day (SD) conditions that could be complemented by introducing *PWO1*$_{pro}$*:PWO1-GFP* (Figures 3A to 3C; Supplemental Figure 3).

The analysis of the morphological phenotypes of *pwo1* mutant alleles showed only mild phenotypes compared with PcG mutants like *clf* or *lhp1 tfl2* (Goodrich et al., 1997; Larsson et al., 1998). Since *PWO1* is a member of a gene family, the expression patterns of the two genes with closest similarity to *PWO1*, *PWO2* and *PWO3*, were analyzed by RT-PCR. RNA from different tissues was isolated, and all three genes showed a largely identical expression pattern in all tissues that were tested (Figure 3D). While T-DNA insertions in *PWO2* and *PWO3* and double mutant combinations *pwo1 pwo2*, *pwo1 pwo3*, and *pwo2 pwo3* resulted in mild morphological phenotypes compared with the wild type, *pwo1-1 pwo2-2 pwo3-2* triple mutants exhibited a dramatic seedling phenotype (Figures 3E and 3G to 3K; Supplemental Figure 2). The triple mutants showed a termination of the apical root and shoot meristems soon after germination and accumulation of anthocyanins in the shoot tissues (Figures 3E and 3G to 3K). Most seedlings died by 14 d after germination (DAG), lacked chlorophyll, and appeared brownish or translucent. Analysis of the triple mutants by scanning electron microscopy uncovered that epidermal cells of the triple mutants are collapsed by around 14 DAG. These cells appeared noncollapsed at 7 DAG, suggesting that this phenotype occurred postembryonically (Figures 3L to 3N). *pwo1-1 pwo2-2 pwo3-2* triple mutants rarely produced leaf-like organs, instead producing needle-like organs that usually lacked trichomes (Figure 3). To check whether this phenotype depends on

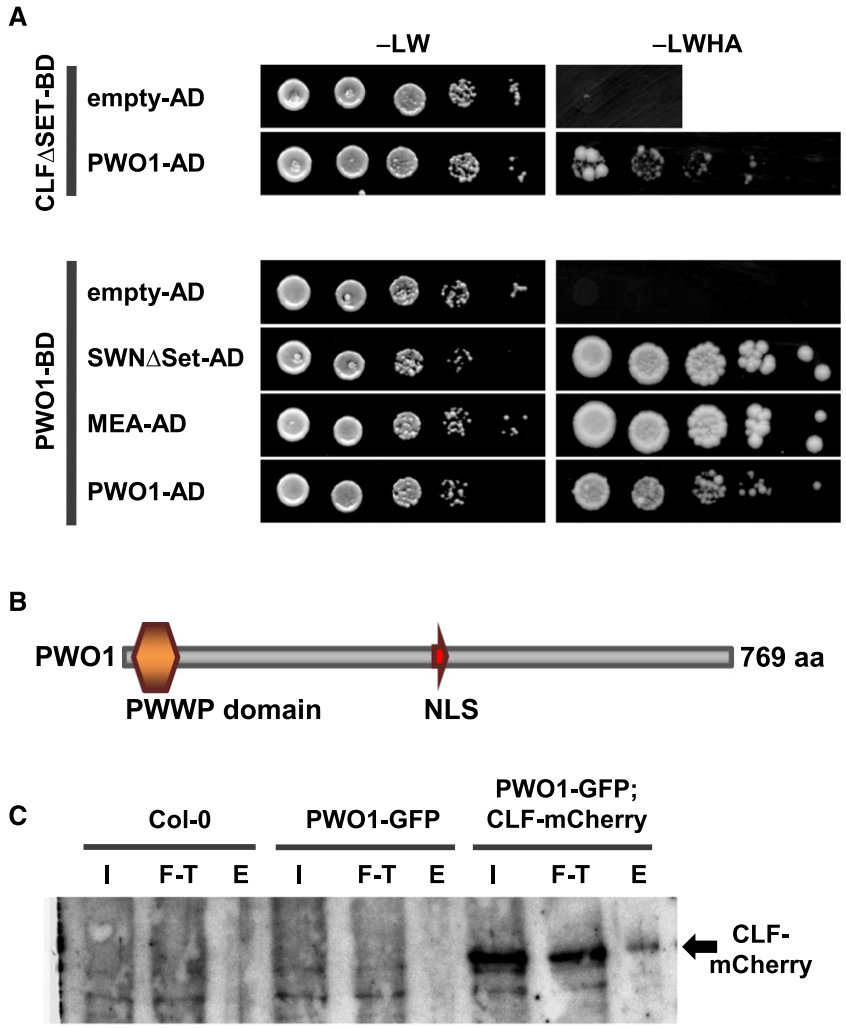

Figure 1. Interaction of PWO1 with PRC2 Members.

(A) Yeast-two hybrid analyses detect an interaction of PWO1 with CLF, SWN, and MEA and PWO1 homodimerization. Yeast cells containing the various combinations were grown on medium selecting for plasmids (−LW; −leucine, tryptophan) or for reporter gene activation (−LWAH; adenine, histidine). Serial dilutions are shown. BD, GAL4-DNA binding fusion; AD, GAL4-DNA-activation domain fusion. For CLF and SWN, constructs lacking the SET domain were taken (ΔSET).
(B) Schematic presentation of the predicted PWO1 protein. PWWP, proline-tryptophan-tryptophan-proline domain.
(C) Immunoblot derived from coimmunoprecipitation of PWO1 and CLF from stable Arabidopsis transgenic lines. Immunoprecipitation was performed with anti-GFP antibodies; detection was with anti-mCherry antibodies. I, input; F-T, flow-through; E, eluate.

PWO genes, we introduced $PWO1_{pro}$:*PWO1-GFP* or $PWO3_{pro}$:*PWO3-GUS* transgenes in the triple mutants. Both transgenes fully rescued the triple mutant phenotype (Figure 3F; Supplemental Figure 2). Collectively, our analyses uncover an essential role for the *PWO* gene family in postembryonic growth and in maintenance of both root and shoot meristems; however, this function is masked by the overlapping functions of *PWO1*, *PWO2*, and *PWO3*.

PWO1 Interacts Genetically with *CLF* and Regulates Expression of PcG Target Genes

The physical interaction of PWO1 and CLF suggested that PWO1 and CLF have overlapping functions during Arabidopsis development. To test this, we generated *pwo1-1 clf-28* double mutants, which resulted in a strong enhancement of the *clf* phenotype: a severe reduction of plant size, very strong upwards leaf curling, and daylength-independent early flowering, suggesting a genetic interaction of *PWO1* and *CLF* (Figures 4A to 4C). *pwo1* mutants strongly enhanced the *clf* phenotype even in SD conditions, where the *clf* leaf phenotype is largely suppressed (Supplemental Figure 3).

To reveal the genes causal for enhancement of the *clf* mutant phenotype, we tested expression of the MADS box genes *FLC*, *FLOWERING LOCUS T* (*FT*), *AGAMOUS* (*AG*) and *SEPALLATA3* (*SEP3*) in *pwo1* single and *pwo1 clf* double mutants. Ectopic expression of *AG* and *SEP3* is largely responsible for the *clf* mutant phenotype, while loss of *FLC* enhances it (Goodrich et al., 1997; Jiang et al., 2008; Lopez-Vernaza et al., 2012). Consistent

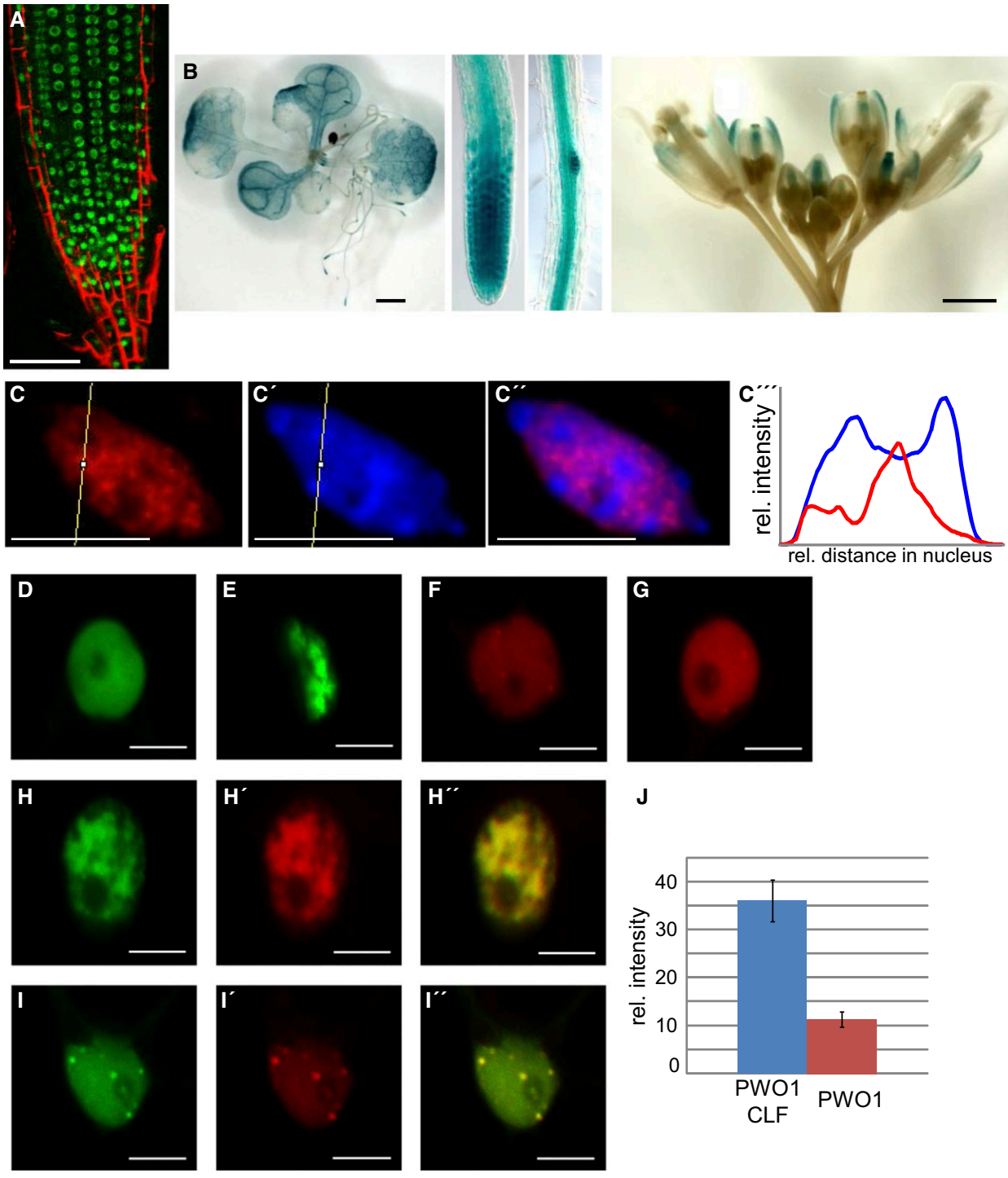

Figure 2. PWO1 Localization, Expression Pattern, and Colocalization with CLF.

(A) *PWO1*$_{pro}$*:PWO1-GFP* reveals PWO1 nuclear localization and expression in most cells of the root tip.
(B) *PWO1*$_{pro}$*:PWO1-GUS* line. GUS staining is detected in seedlings, root tips, root vasculature, and inflorescences.
(C) to **(C′′′)** Immunofluorescence of nucleus isolated from *PWO1*$_{pro}$*:PWO1-GFP* seedlings, stained with anti-GFP **(C)** and DAPI **(C′)**; **(C′′)** is merge of **(C)** and **(C′)**; **(C′′′)** profiles of anti-GFP (red) and DAPI (blue) fluorescence intensities through the yellow line in **(C)** and **(C′)**.
(D) to **(I′′)** Transient expression in *N. benthamiana* leaf epidermal cells. Expression was induced with 2 μM β-estradiol for at least 5 h. *i35S*$_{pro}$*:GFP-CLF* (**[D]** and **[E]**), *i35S*$_{pro}$*:PWO1-mCherry* (**[F]** and **[G]**), and coexpression of *i35S*$_{pro}$*:GFP-CLF* and *i35S*$_{pro}$*:PWO1-mCherry* (**[H]** and **[I]**). **(H′′)** and **(I′′)** are merges of the two channels.
(J) Intensity profiles of speckles in *i35S*$_{pro}$*:PWO1-mCherry* tobacco nuclei (n = 6) and nuclei cotransformed with *i35S*$_{pro}$*:GFP-CLF* and *i35S*$_{pro}$*:PWO1-mCherry* (n = 6).
Bars = 50 μm in **(A)**, 1 mm in **(B)**, 5 μm in **(C)**, and 10 μm in **(D)** to **(I)**.

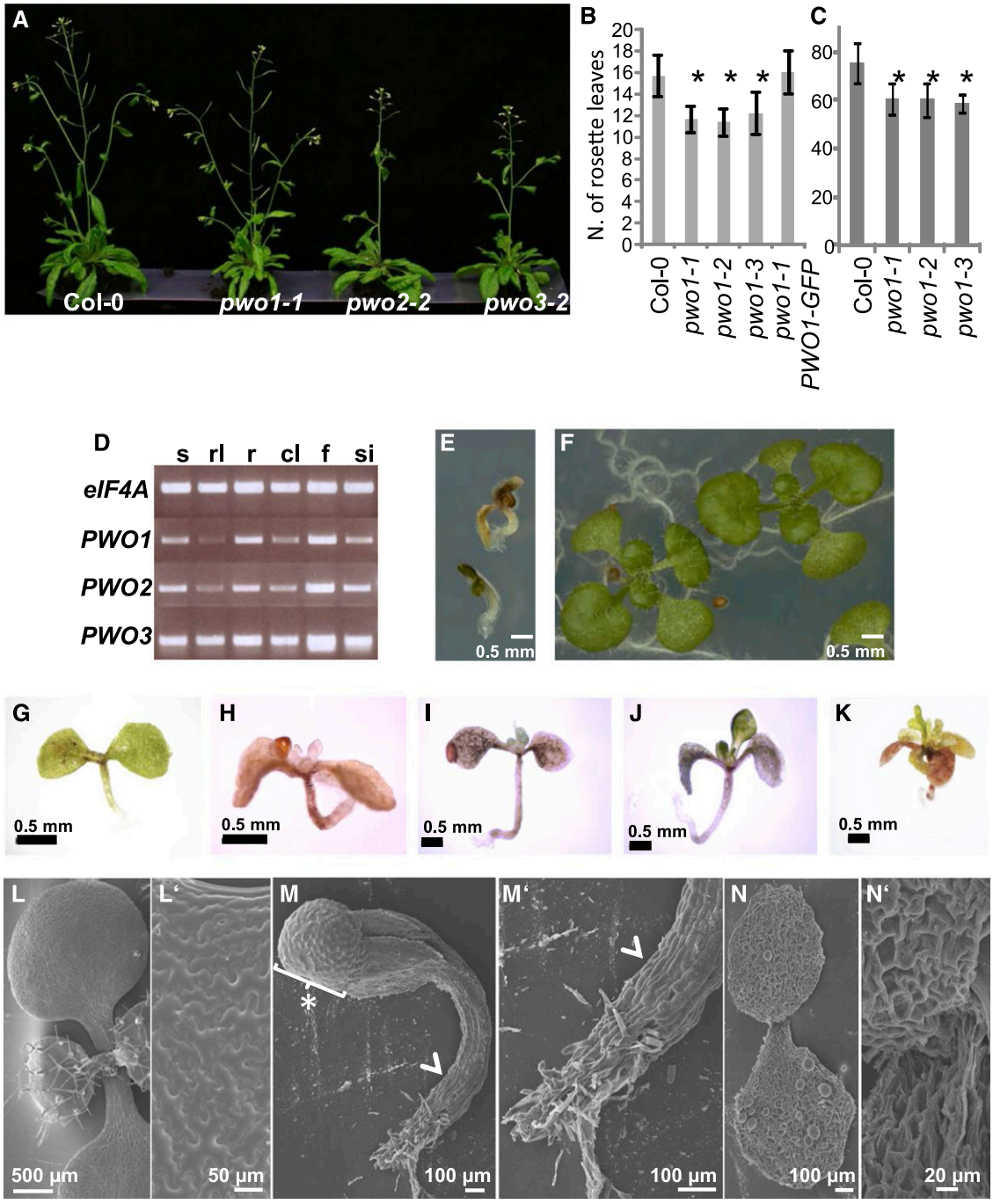

Figure 3. Developmental Analyses of *pwo1*, *pwo2*, and *pwo3* Single and *pwo1/2/3* Triple Mutants.

(A) Growth phenotype of wild-type, *pwo1-1*, *pwo2-2*, and *pwo3-2* plants (30 DAG).
(B) and **(C)** Flowering time analyses of wild-type Col-0, *pwo1* alleles, and *pwo1-1 PWO1*$_{pro}$*:PWO1-GFP* (*pwo1-1* PWO1-GFP) in LD **(B)** and SD **(C)**; *x* axes indicate number of rosette leaves at time of bolting; $n \geq 19$. Asterisks indicate a significantly different number of rosette leaves compared with Col-0 (Student's *t* test, $P < 0.01$).
(D) Expression analyses (RT-PCR) of *PWO1*, *PWO2*, and *PWO3* expression in seedlings (s), rosette leaves (rl), roots (r), cauline leaves (cl), flowers (f), and siliques (si); *eIF4A* was used as reference gene.
(E) and **(F)** *pwo1-1 pwo2-2 pwo3-2* triple mutants show seedling lethality **(E)**, which is rescued by a *PWO1*$_{pro}$*:PWO1-GFP* transgene **(F)**. Plants are shown at 14 DAG.
(G) to **(K)** Various classes of seedling phenotypes of *pwo1/2/3* triple mutants (10–21 DAG).

with daylength-independent early flowering of *pwo1* and *flc* mutants (Figures 3B and 3C) (Michaels and Amasino, 1999; Sheldon et al., 1999), *FLC* was hardly detectable in *pwo1* (Figure 5A), whereas *FT* expression was not affected (Supplemental Figure 4). In addition, *pwo1 flc* double mutants showed similar flowering time as each single mutant, suggesting that *flc* is epistatic to *pwo1* in LD and SD conditions in terms of flowering time control (Figure 4C; Supplemental Figure 3). As an introduction of *flc-3* in the *clf-28* mutant background leads to an enhancement of the early flowering and leaf curling phenotype (Lopez-Vernaza et al., 2012), the enhancement of *clf* by *pwo1* may be largely due to lower levels of *FLC* expression. Indeed, *pwo1-1 clf-28* mutants showed similar misregulation of *FT* and flowered at the same time as *flc-3 clf-28*, indicating that the decrease of *FLC* expression in the *pwo1-1* mutant might be responsible for enhancing the *clf-28* flowering phenotype (Figure 3; Supplemental Figure 4). However, *pwo1-1 clf-28* mutants showed a stronger enhancement of the *clf-28* phenotype with respect to plant size and leaf curling than the *flc-3 clf-28* double mutants (Figure 4B), suggesting that misregulation of additional genes besides *FLC* is causal for enhancement of *clf-28* by *pwo1-1*. We therefore analyzed expression of the PcG target genes *AG* and *SEP3*, whose misexpression is largely responsible for the *clf* mutant phenotype (Goodrich et al., 1997; Lopez-Vernaza et al., 2012). Importantly, *AG* and *SEP3* showed a similar misexpression in *flc-3 clf-28* compared with the *clf-28* single mutant, while in *pwo1-1 clf-28*, *AG* was slightly and *SEP3* was more strongly expressed than in *clf-28* (Figure 5A). To reveal whether changes in PcG target gene expression are correlated with reduced levels of the PRC2 mark H3K27me3, we performed chromatin immunoprecipitation (ChIP) experiments in Col-0 and in *pwo1* and *pwo1 pwo3* mutants. While H3K27me3 occupancy was significantly reduced at *SEP3*, *AG*, and *FUSCA3* in *pwo1* mutants compared with Col-0 (Figure 5B; Supplemental Figure 5), *FLC* H3K27me3 levels were only affected in *pwo1 pwo3* double but not in *pwo1* single mutants. However, we observed an even stronger reduction in H3 occupancy at all tested loci, suggesting that PWO1 is rather required for full nucleosomal levels than for high levels of H3K27me3. In summary, *SEP3* and *AG* upregulation and *FLC* downregulation in *pwo1-1 clf-28* double mutants compared with *clf-28* single mutants largely explain the double mutant phenotype. In addition, PWO1 represses *SEP3* at least partially independently of FLC and regulates H3K27me3/H3 enrichment at the tested loci.

The PWWP Domain of PWO1 Is Required for Nuclear Speckle Formation in *N. benthamiana* and for Interaction with H3

PWO1 contains a putative chromatin "reading" domain, the PWWP domain (Figure 1; Supplemental Figure 1), which has been shown to target various proteins to chromatin (Dhayalan et al., 2010; Maltby et al., 2012; Wang et al., 2009); therefore, this domain might have a similar function in the PWO1 protein. As PWO1 partially localizes to nuclear speckles (Figures 2F, 2G, and 2I), we asked whether the PWWP domain may be required for subnuclear targeting. We therefore generated N-terminal (lacking the PWWP domain) and C-terminal deletions of PWO1 fused to GFP, which both contained the predicted NLS (*i35S$_{pro}$:PWO1ΔPWWP-GFP* and *i35S$_{pro}$:PWO1ΔC-GFP*), and compared subcellular localization with the full-length PWO1 cDNA fused to GFP (*i35S$_{pro}$:PWO1cDNA-GFP*) in transient expression assays in *N. benthamiana* (Figures 6A to 6C). Although fewer speckles were visible in C-terminally truncated PWO1 constructs (Figure 6B), only complete loss of speckle formation and partly cytoplasmic localization were observed with the PWO1 construct lacking the PWWP domain (Figure 6C).

As PWWP domains have been shown to confer binding to histones, for example in the mammalian de novo DNA methyltransferase DNMT3A (*Mus musculus*) or the Pdp1 protein from *Schizosaccharomyces pombe* (Dhayalan et al., 2010; Qiu et al., 2002; Wang et al., 2009), we next sought to determine whether the PWWP domain of PWO1 (PWO1-PWWP) also interacts with histones. An alignment of the predicted PWO1 PWWP domain with those of the Arabidopsis proteins PWO2, PWO3, and ATX1, mouse DNMT3A, DNMT3B, and MSH6, human NSD2, and *S. pombe* Pdp1 proteins detected conservation of several important residues, which are predominantly hydrophobic (Supplemental Figure 6). To further characterize the binding ability of the PWWP domain, the full PWO1 cDNA or a shorter fragment corresponding to the N-terminal half of the protein was fused to GST and purified from *Escherichia coli* to assay binding to H3 by coimmunoprecipitation experiments with anti-H3 antibodies. Both proteins were able to bind H3, indicating that the N-terminal part of the protein, which contains the PWWP domain, is sufficient to confer binding to H3 (Figures6 6D and F). It has been shown that direct interaction of PWWP domains to histones occurs through a hydrophobic pocket formed by three aromatic amino acids (Qin and Min, 2014). PWO1-PWWP contains a partial hydrophobic pocket formed by two tryptophan residues (Supplemental Figure 6). Strikingly, the point mutation of one of them, W63, to alanine (PWO1-W63A), decreases PWO1-H3 interaction in vitro (Figure 6E).

To analyze the role of the PWWP domain in PWO1's functions, the *pwo1 pwo2 pwo3* triple mutant was transformed with a construct carrying the W63A point mutation in this domain (*PWO1$_{pro}$:PWO1$_{W63A}$-GFP*) and expression and nuclear localization of PWO1$_{W63A}$-GFP was confirmed in vivo (Supplemental Figure 7). The phenotypic analysis of two independent *PWO1$_{pro}$:PWO1$_{W63A}$-GFP pwo1 pwo2 pwo3* transgenic lines showed a partial complementation so that cotyledons and roots appeared more normal than in the triple mutants, i.e., hypocotyls and cotyledons were more elongated and cotyledons accumulated chlorophyll.

Figure 3. (continued).

(L) and **(L′)** Scanning electron microscopy analyses of wild-type seedling (14 DAG; **[L]**) and close-up of cotyledon epidermis **(L′)**.
(M) and **(M′)** *pwo1-1 pwo2-2 pwo3-2* seedling at 14 DAG **(M)**; note noncollapsed epidermal cells (arrowhead). Asterisk with brackets indicates seed coat. **(M′)** is a close-up of root tip in **(H)**.
(N) and **(N′)** *pwo1-1 pwo2-2 pwo3-2* seedling at 21 DAG **(N)**; note collapsed epidermal cells; **(N′)** is a close-up of SAM showing lack of leaf primordia.

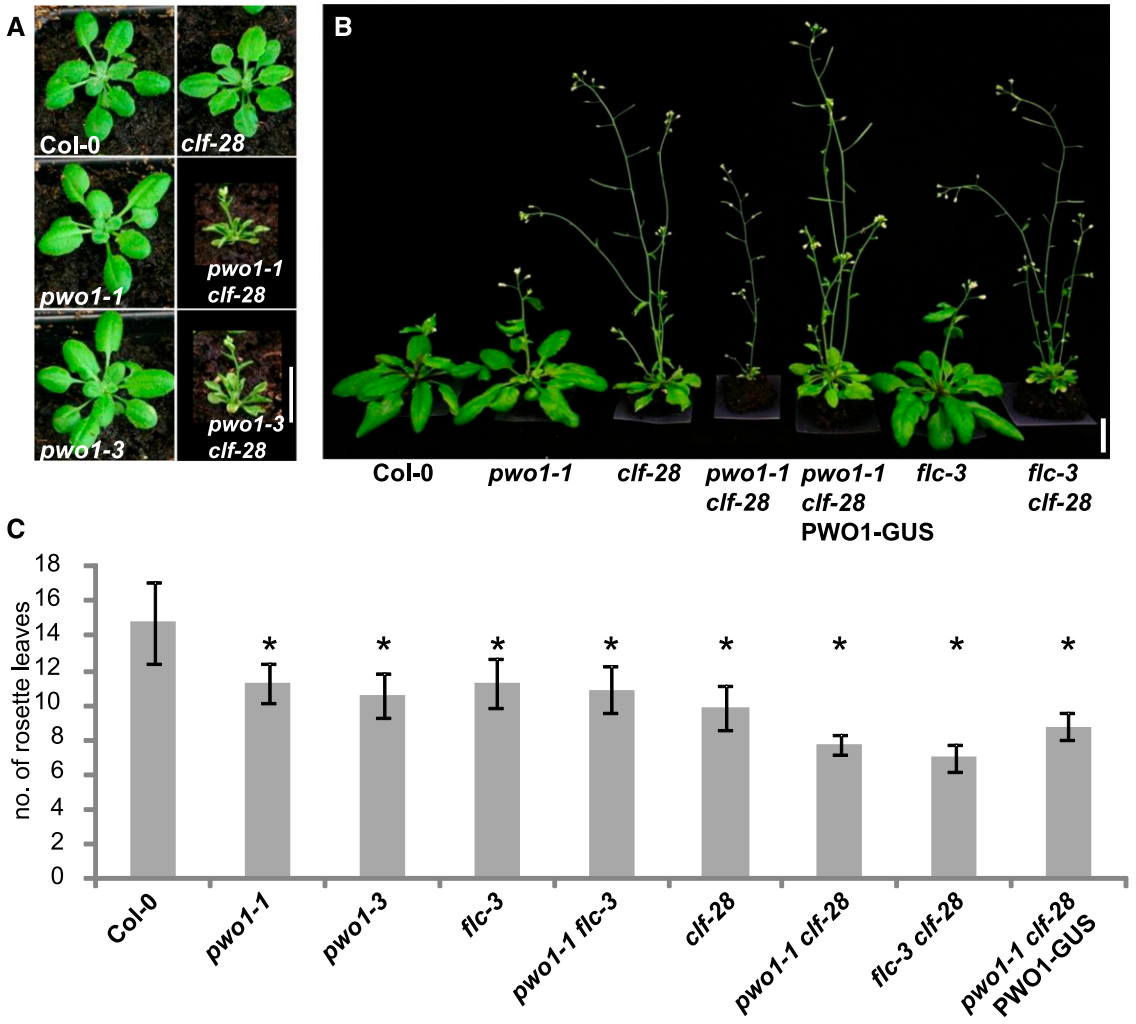

Figure 4. Genetic Interaction of *pwo1*, *clf*, and *flc* and Regulation of PcG Target Genes by PWO1.

(A) *pwo1* alleles enhance the *clf* mutant phenotype (plants at 21 DAG, grown in LD conditions).
(B) *pwo1* and *flc*-3 enhance the *clf-28* phenotype, but *pwo1-1 clf-28* double mutants have a stronger phenotype than *flc-3 clf-28* (plants at 30 DAG, LD conditions).
(C) Flowering time analyses of plants grown in LD. Loss of *PWO1* and *FLC* similarly enhance early flowering of *clf-28*, while *pwo1-1*, *flc-3*, and *pwo1-1 flc-3* are similarly early flowering. $n \geq 23$ (except for *clf-28 flc-3*; $n = 3$). Asterisks indicate significantly different number of rosette leaves compared with Col-0 (Student's *t* test, $P < 0.001$). Rosette leaf numbers of *pwo1-1*, *pwo1-3*, *flc-3*, and *pwo1-1 flc-3* are not significantly different to each other (Student's *t* test, $P > 0.1$).

However, the shoot apical meristem (SAM) seemed initially reduced and then produced callus-like tissue from which leaves eventually developed (Figures 6G to 6I).

Thus, the PWWP domain of PWO1 appears to be essential for its interaction with H3. In addition, PWO1-H3 interaction might be required for PWO1 nuclear localization and formation of nuclear speckles in *N. benthamiana* and for full PWO1 activity in Arabidopsis.

The PWO1 PWWP Domain Binds to Histone Peptides Lacking H3S28 Phosphorylation

To analyze whether the PWO1 PWWP domain confers binding to posttranslationally modified histones, we fused it to GST, expressed it in *E. coli*, and purified the fusion protein. The GST-PWO1-PWWP fusion protein was then incubated with the Modified histone peptide array harboring different combinations of naturally occurring histone modifications on histone peptides (Bock et al., 2011). The GST-PWO1-PWWP fusion protein bound rather nonspecifically to histone peptides and modified histone peptides; however, binding was specifically inhibited by phosphorylation of H3S28 (Figure 7A). Importantly, non-histone peptides were not bound and binding was not disrupted by H3S10 phosphorylation, which lies in a similar sequence context as H3S28 (N-ARKS-C). This suggests that loss of binding is not only caused by an increase in negative charge, but also depends on the sequence context N- or C-terminal to the ARKS sequence.

The binding capacity of GST-PWO1-PWWP to unmodified and modified histone H3 peptides was then independently

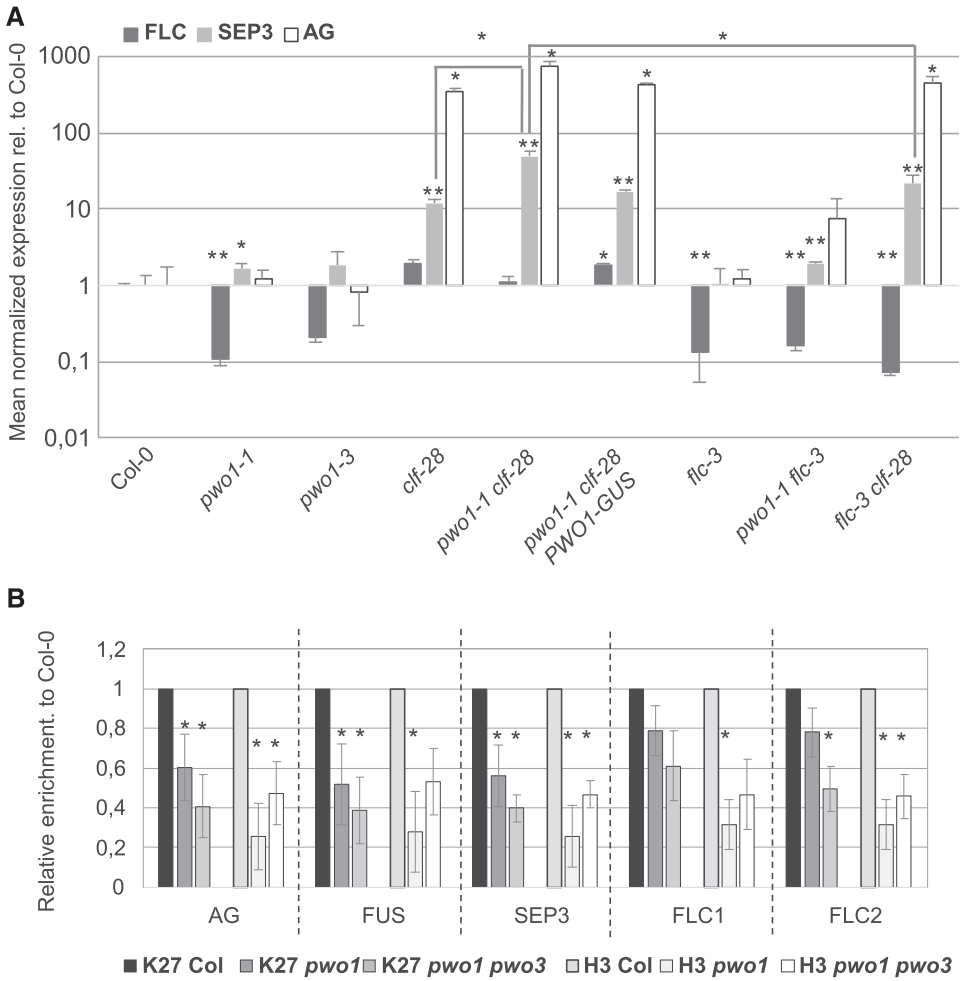

Figure 5. Expression and Chromatin Analyses in *pwo* Mutants.

(A) RT-qPCR analyses of the PcG target genes *FLC*, *SEP3*, and *AG* in various mutant backgrounds. Pools of seedlings grown in LD were harvested at 10 DAG. Asterisks indicate significant difference (*P < 0.01 and **P < 0.001, Student's *t* test). Significance was analyzed in comparison to the wild type (Col-0) or as indicated by brackets. Error bars indicate SE of three biological replicates, grown and harvested independently. Note logarithmic scaling.
(B) ChIP in wild-type, *pwo1*, and *pwo1 pwo3* mutants using antibodies against H3K27me3 and H3. Ten-day-old, LD-grown seedlings were analyzed. Results were normalized to measurements for Col-0 and represent the mean of three biological replicates (error bars depict SE), and asterisks indicate significantly different enrichment compared with Col-0 (n.s., P > 0.05; *P < 0.05, Student's *t* test). See Supplemental Figure 4 for full data set, including control regions devoid of H3K27me3 and % IP values.

demonstrated in vitro in peptide pull-down experiments. As revealed in the peptide array, H3 (amino acids 21–44) and H3K27me3 peptides precipitated the GST-PWO1-PWWP fusion protein; however, binding was strongly reduced by H3S28 phosphorylation (Figures 7B and 7C). While GST alone was not able to bind to the biotinylated peptides, a GST fusion protein with the CHROMO domain of TFL2/LHP (GST-TFL2-CHROMO) showed in vitro binding ability to H3 peptides trimethylated at K27, consistent with previously published data (Turck et al., 2007; Zhang et al., 2007).

Although currently the impact of H3S28 phosphorylation on PcG-mediated H3K27me3 and gene silencing has not been studied in plants, a role for H3S28p in antagonizing PcG silencing has recently been uncovered in animals (Gehani et al., 2010; Lau and Cheung, 2011). As H3S28 is adjacent to the PRC2-modified H3K27 also in plants, a similar mechanism of PcG displacement may occur here as well.

DISCUSSION

PWO1 Recruits Arabidopsis PcG Proteins to Subnuclear Speckles

Plant genomes contain a multitude of genes with similarity to chromatin regulators. However, only a few plant-specific components of chromatin and PcG complexes have been identified so far. These may substitute for nonconserved proteins and contribute to key processes in epigenetic gene regulation including recruitment of the complexes to their target genes and inheritance of the epigenetic state through mitosis and/or meiosis. Alternatively,

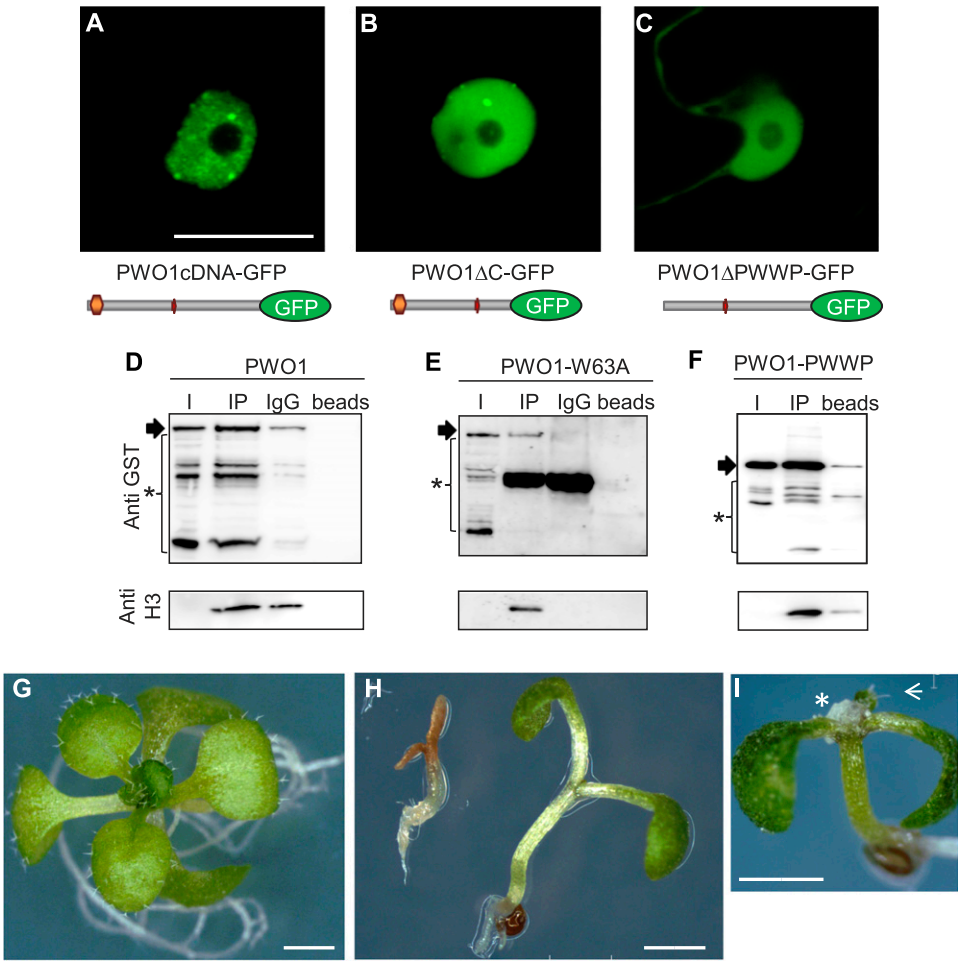

Figure 6. The PWWP Domain of PWO1 Is Required for Nuclear Speckle Formation and Interaction with H3.

(A) to **(C)** Transient expression of PWO1-GFP variants in *N. benthamiana* leaf epidermal cells. *i35S$_{pro}$:PWO1cDNA-GFP* **(A)**, *i35S$_{pro}$:PWO1ΔC-GFP* **(B)**, and *i35S$_{pro}$:PWO1ΔPWWP-GFP* **(C)**. Expression was induced with 5 μM β-estradiol for 5 h. Bar = 20 μm.

(D) to **(F)** Coimmunoprecipitation of H3 with the full cDNA of PWO1 fused to GST **(D)**, with a mutated version of PWO1 carrying a W63A point mutation **(E)** or the N-terminal part of PWO1 **(F)**. Two percent of input was run in the gel as loading control. I, input; IgG, beads coupled to IgG as negative control; beads, uncoupled beads.

(G) to **(I)** Comparison of *pwo1 pwo2 pwo3* mutants carrying different constructs: **(G)** *pwo1 pwo2 pwo3 PWO1$_{pro}$:PWO1-GFP*; **(H)** left, *pwo1 pwo2 pwo3* and right, *pwo1 pwo2 pwo3 PWO1 $_{pro}$:PWO1$_{W63A}$-GFP*; **(I)** *pwo1 pwo2 pwo3 PWO1 $_{pro}$:PWO1$_{W63A}$-GFP* showing callus-like tissue in the SAM (asterisk) and leaf primordium with trichomes (arrow), which were not observed in *pwo1 pwo2 pwo3* triple mutants. **(G)** and **(H)** are 2-week-old plants, and **(I)** is a 3-week-old plant grown in tissue culture in LD photoperiod. Bars = 1 mm.

they may fulfill plant-specific roles that may have evolved to accommodate the different lifecycles of plants and animals.

In this study, we aimed to identify interaction partners of the PRC2 protein CLF and focused on plant-specific components with putative chromatin "reading" domains. Among other proteins, we identified the PWWP-domain protein PWO1, which interacts with all three histone methyltransferase subunits of the Arabidopsis PRC2, CLF, SWN, and MEA, in yeast. PWWP domains belong to the "royal family" of domains that have diverse functions in chromatin regulation and have been shown to bind to DNA or (posttranslationally modified) histones (Dhayalan et al., 2010; Maurer-Stroh et al., 2003; Qin and Min, 2014; Qiu et al., 2002; Wang et al., 2009). PWWP domains are found in a diverse range of proteins in uni- and multicellular organisms including Arabidopsis whose genome encodes at least 19 PWWP-domain proteins (16 identified by Alvarez-Venegas and Avramova [2012] plus the three in this study). Similar to PcG proteins, *PWO1* is expressed in diverse tissues and localizes to euchromatic regions in the nucleus. Interestingly, we revealed that PWO1 localizes to nuclear speckles when expressed transiently in *N. benthamiana* and stably in Arabidopsis; however, the distribution of the speckles in Arabidopsis seemed more uniform despite their absence from chromocenters. CLF and PWO1 influence each other's subnuclear localization in tobacco: While CLF only localizes to nuclear speckles in the presence of PWO1, PWO1 is only observed in larger nuclear patches when coexpressed with CLF.

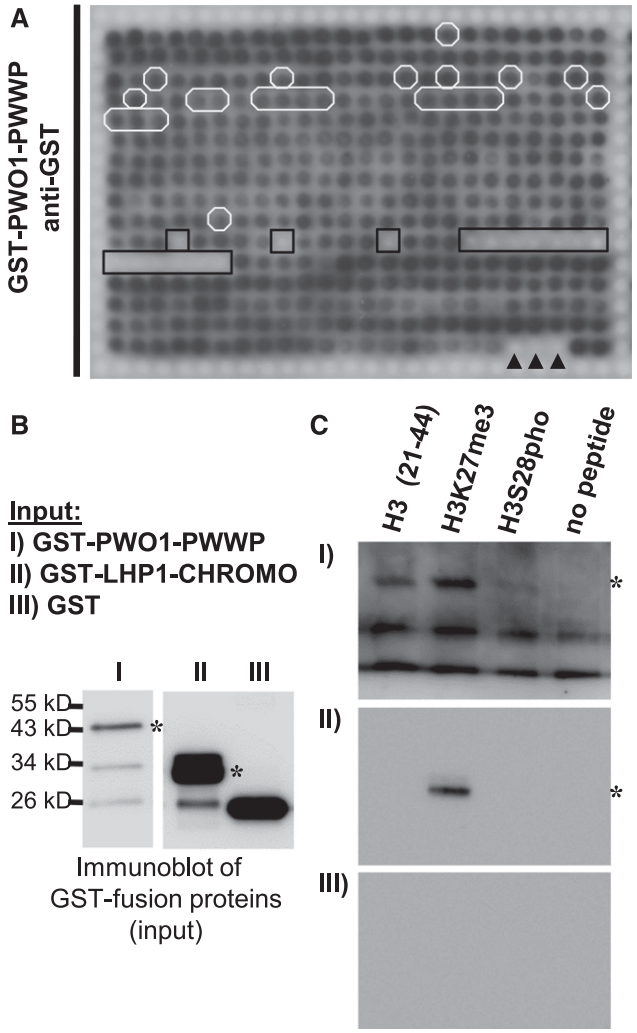

Figure 7. The PWO1 PWWP Domain Binds to Histone Peptides Lacking H3S28 Phosphorylation.

(A) Binding of the PWO1 PWWP domain (GST-PWO1-PWWP) to peptide arrays containing 384 different peptides. Peptides containing H3S10p are in white circles and ovals, and peptides carrying H3S28p are in black boxes. Arrowheads indicate non-histone peptides. For a detailed annotation of all spots, see http://www.activemotif.com/catalog/668/modified-histone-peptide-array.

(B) and **(C)** Confirmation of PWO1-PWWP histone binding by peptide pull-down analyses. GST fusion proteins were separated by polyacrylamide gel electrophoresis and blotted to a nitrocellulose membrane **(B)**. Fusion proteins were detected with anti-GST antibody staining **(C)**. (I) to (III) Fusion proteins were incubated with biotinylated histone peptides and precipitated with Streptavidin beads. Pulled-down proteins were separated by polyacrylamide gel electrophoresis, blotted to a nitrocellulose membrane, and detected with anti-GST antibody staining. Asterisks indicate fusion proteins in **(B)** and **(C)**. Faster migrating bands in (I) are GST-PWO1 degradation products.

Nuclear speckle formation depends on the PWO1 PWWP domain, suggesting that chromatin targeting by the PWWP domain may precede speckle formation. The identity of the speckles is currently unclear (Del Prete et al., 2015), but other PcG proteins like VRN2, LHP1/TFL2, and EMF1 also were found to localize to nuclear speckles when expressed transiently in *N. benthamiana*, *Nicotiana tabacum*, or onion (*Allium cepa*) epidermal cells (Calonje et al., 2008; Gaudin et al., 2001; Gendall et al., 2001; Libault et al., 2005; Zemach et al., 2006). Nevertheless, as the speckles are not clearly detected in Arabidopsis, we cannot exclude that the transient expression of PWO1 in a heterologous system may favor speckle formation. It is also possible that putative PWO1 speckles in Arabidopsis are much smaller than the ones detected in *N. benthamiana*; however, examining this possibility would require higher resolution microscopy. Nevertheless, Drosophila and mammalian PRC1 proteins are found in so-called PcG bodies, which are observed as nuclear speckles whose number and size vary depending on the cell type (Pirrotta and Li, 2012). While the mammalian ortholog of CLF, ENHANCER OF ZESTE HOMOLOG2 (EZH2), is required for PcG body formation (Hernández-Muñoz et al., 2005), EZH2 is not found in the bodies (Sewalt et al., 1998). However, there is still no clear evidence for PcG bodies in plants and further experiments will be required to determine whether PWO1-CLF speckles correspond with clustering of both proteins and interaction with PcG target genes as observed in Drosophila (Bantignies et al., 2011). We also found that PWO1 may form homodimers that could contribute to subnuclear speckle formation and possibly polymerization as shown for mammalian polyhomeotic homolog 2 (Isono et al., 2013).

Role of the PWO Family in Arabidopsis Development, Flowering Time Control, and PcG Target Gene Regulation

Plant PcG proteins control various developmental processes including flowering time and embryo and seedling development (Mozgova et al., 2015). Similar to *clf* and *emf* mutants, *pwo1* shows an early flowering phenotype in which misexpression of some PcG target genes seems to play an important role. In contrast to *clf* and other PRC2 mutants, *FLC* expression is lower in *pwo1* (Jiang et al., 2008; Lopez-Vernaza et al., 2012), while other flower-specific PcG target genes are ectopically expressed in *pwo1* or show enhanced ectopic expression in *clf pwo1* mutants. Similar expression patterns which include reduced levels of *FLC* are also observed in *incurvata2*, *blister*, *chr11/17*, and *ringlet* mutants (Barrero et al., 2007; Li et al., 2012; Schatlowski et al., 2010), whose wild-type products all show a physical and/or genetic interaction with PcG proteins or mutants, respectively. Thus, these and the PWO1 proteins may have a dual function as activators and repressors of distinct PcG target genes. Alternatively, the effect on *FLC* may be indirect and these proteins may repress a repressor of *FLC*, similar to what has been reported for the PcG target gene *FT* whose expression is downregulated in strong PcG mutants (Farrona et al., 2011). Our chromatin analyses suggest that the observed reduction in H3K27me3 occupancy in *pwo1* mutants is largely due to a reduction in H3 occupancy, suggesting that *PWO1* is not required for H3K27me3 activity of PRC2. However, it may be involved in compaction of PcG target chromatin, either to facilitate PRC2 H3K27 methyltransferase activity or to compact nucleosomes after the H3K27me3 mark has been set. PWO1's general affinity for histones is consistent with this function, and it will be important to study interactions of PWO1 with chromatin remodeling components. In addition, it remains to be elucidated whether

the decrease in H3 occupancy occurs throughout the genome or specifically at PcG target genes.

While *pwo1* mutants are similar in size to the wild type, they strongly enhance *clf* mutants resulting in small plants with severe leaf curling and very early flowering. However, the full function of PWO1 in plant development is masked by the redundancy with its two homologous proteins PWO2 and PWO3. The triple mutants show shoot and root meristem arrest and produce no or severely affected postembryonic organs and die a few weeks after germination, indicating their essential role for development. Strong PcG mutants like the *clf swn* double mutant show a somewhat weaker phenotype as they keep on proliferating after germination and produce leaf and root tissue (Chanvivattana et al., 2004). This difference in phenotype may be explained by different PcG target gene activation in *pwo1/2/3* and PRC2 mutants or a PcG independent role of the PWO family. Nevertheless, the severe *pwo1/2/3* mutant phenotype reveals an essential role for the PWO family in preventing premature differentiation and maintaining meristematic activity.

PWO1 Interacts with H3 through Its Conserved PWWP Domain and May Recruit PcG Proteins to Unphosphorylated H3S28 Tails

PWWP domains are found in numerous proteins and belong to the "royal family" of chromatin readers (Maurer-Stroh et al., 2003). Several PWWP-domain proteins bind to histones; for instance, the PWWP domain of DNMT3A interacts with H3 and *S. pombe* Pdp1's PWWP domain binds H4. Other PWWP-domain proteins, such as DNMT3B, interact with DNA (Dhayalan et al., 2010; Qiu et al., 2002; Wang et al., 2009).

We revealed that PWO1 interacts with H3 in vitro and that a fragment of the protein containing the PWWP domain is sufficient to allow this interaction. Binding of PWWP domains to histones occurs through a hydrophobic pocket formed by three aromatic residues that in many cases have been shown to specifically recognize methyl-lysine residues on the histone tail (Qin and Min, 2014). Sequence analysis of the PWWP in PWO1-3 showed that the domain in these proteins has a partial hydrophobic domain in which the first aromatic residue has been substituted by glycine. Other proteins with an incomplete aromatic cage, such as the Retinoblastoma Binding Protein 1, do not show specificity for methylated residues (Gong et al., 2012), indicating that a different mechanism might be also involved in PWO1-H3 binding.

Further demonstration of the importance of the PWWP domain of PWO1 with H3 was shown through the point mutation of the W63 residue of PWO1's semiaromatic cage. This amino acid has been described to form part of the groove that interacts with specific residues in the N-terminal tail of H3 (Qin and Min, 2014). When this residue was mutated to alanine in PWO1-PWWP, a decrease of the binding of the domain to H3 was observed in vitro. Mutation of the corresponding residue in the Pdp1 protein of *S. pombe* strongly disrupted in vitro binding of Pdp1 to H4K20me3 (Wang et al., 2009). Therefore, our data indicate that other residues in PWO1's PWWP may also play an important role in the interaction with H3 under the tested conditions. This hypothesis was also supported by our in vivo results for complementation of the *pwo1 pwo2 pwo3* mutants with the version of PWO1 carrying the W63A point mutation. The experiments showed that PWO1-W63A was not able to fully complement the triple mutants, probably indicating a partial activity of the mutated PWWP domain and of the protein carrying this mutation. This residue might be especially important for the function of PWO1 in maintaining meristematic activity, considering that the SAM was the organ most strongly affected in the $PWO1_{pro}$:$PWO1_{W63A}$-*GFP pwo1 pwo2 pwo3* plants.

We further revealed that, at least in vitro, PWO1 does not have a preference for posttranslationally modified histone peptides; however, the interaction is inhibited by phosphorylation of H3S28. A related function has been shown for a cysteine-rich domain of DNMT3L, which specifically recognizes nonmethylated H3K4 (Ooi et al., 2007).

Currently there is limited information available on the function of H3S28p or H3K27me3S28p in plants. H3S28p and H3S10p accumulate during mitosis and meiosis in diverse plant species, but are hardly detectable in interphase nuclei (Gernand et al., 2003), similar to what has been observed in mammals (Goto et al., 1999). Importantly, H3K27me3S28p was shown to counteract PcG repression upon stress induction (Gehani et al., 2010; Lau and Cheung, 2011), potentially providing a powerful way of quickly and transiently relieving PcG repression. PWO1 may therefore be involved in stabilizing the PRC2-Histone interaction, which can be disrupted by phosphorylation of H3S28.

In conclusion, PWO1 (and possibly also PWO2 and PWO3) may interact with PcG proteins to recruit them to subnuclear speckles and to mediate full H3/nucleosomal compaction. In this activity, its PWWP domain may act as a key element in the interaction of PWO1 with the chromatin, possibly by its ability to interact with histones. Accumulation of H3S28p during stress treatment and/or cell division may lead to displacement of PWO1 and associated PcG proteins and release of PcG target gene silencing. The *PWO1/2/3* genes are essential for proper cell division and maintenance of stem cells as lack of their function causes early seedling lethality with root and shoot meristem arrest. Whether this is a result of improper recruitment of PcG proteins is an interesting possibility to explore in the future.

METHODS

Biological Material

The *PWO1* T-DNA insertion lines were identified using the SIGNAL database (http://signal.salk.edu/cgi-bin/tdnaexpress) and provided by the Nottingham Arabidopsis Stock Centre: *pwo1-1* (N815951), *pwo1-2* (N420954), *pwo2-2* (N636093), and *pwo3-2* (N836957) (Alonso et al., 2003; Sessions et al., 2002). TILLING (Targeting Induced Local Lesions IN Genomes) mutants were ordered from the Seattle Tilling Project and analyzed (http://tilling.fhcrc.org) (Till et al., 2003). The *pwo1-3* (N93526) allele exhibits a point mutation (R46Stop) leading to a premature stop codon. Homozygous mutants were isolated by PCR-based genotyping (for oligonucleotide sequences, see Supplemental Table 1). For analysis of genetic interactions, crosses were performed with *clf-28* (N639371) and *flc-3* (Michaels and Amasino, 1999). All genotypes used in this study are in the Col-0 background.

Seeds were sterilized and sown on GM media (half-strength Murashige and Skoog medium plus 0.5% sucrose), stratified for 2 d at 4°C, and transferred to soil after 10 to 12 d. Plants were grown at either long-day conditions (16-h-light/8-h-dark cycles at 20°C) or SD conditions (8-h-light/

16-h-dark cycles at 20°C) (light intensity was 120 μmol/m^2/s using RZB LED bulbs Planox Eco 451178.009).

Transformation of *Arabidopsis thaliana* was performed using the floral dip method and the *Agrobacterium tumefaciens* strain GV3101 pMP90 (Clough and Bent, 1998).

Complementation of the *pwo1-1* and *pwo1 pwo2 pwo3* Mutant Phenotype

The *PWO1$_{pro}$:PWO1-GUS* and *PWO1$_{pro}$:PWO1-GFP* constructs where generated by amplification of the genomic locus of *PWO1* including 1534 bp upstream of the transcriptional start site using the following primers: CTAACTTCACAGCACGGCTCTGAGG and TTGAACTCTTCTTCTCTCGTTAAAGGC. The PCR fragment was cloned into the pCR8/GW/TOPO entry vector (Invitrogen) and subsequently cloned into pMDC163 as translational fusion with the uidA gene and into pMDC107 as translational fusion with GFP (Curtis and Grossniklaus, 2003). To create the *PWO1$_{pro}$:PWO1$_{W63A}$-GFP* construct, *PWO1$_{pro}$:PWO1-GFP* was cloned in the pCR8/GW/TOPO entry vector and using primers GTGCTTAGGGATGCGTACAATTTAGAG and ATTAAAATACGAATGCTTTCAGTAATC to introduce the mutation.

Using the floral dip method, *pwo1-1$^{-/-}$ pwo2-2$^{+/-}$ pwo3-2−/−* plants were transformed with Agrobacterium carrying the T-DNA vectors. Plants carrying the transgene were selected on GM medium containing hygromycin (15 mg/mL) and further segregated to obtain the desired genotype.

Phenotypic Analyses and Imaging

Photographs were taken with an AxioCam ICC1 camera (Zeiss) mounted onto a Zeiss Stemi 2000C. For scanning electron microscopy, plant material was treated as described previously (Kwiatkowska, 2004) and scanning electron microscopy was performed using the LEO (Zeiss) microscope and software. For visualization of chromocenters in Arabidopsis PWO1$_{pro}$:PWO1-GFP and PWO1$_{pro}$:PWO1(S63A)-GFP lines, anthers' filaments were mildly fixed in 4% paraformaldehyde under vacuum for 2 min, washed three times with PBS, incubated with propidium iodide solution (1 μg/mL) for 20 min in darkness and again washed three times with PBS. Fluorescence was monitored with a Zeiss LSM 710 confocal laser scanning microscope. Intensity values of fluorescence in particular regions of nuclei were scored afterwards using the Plot Profile feature for intensity profiles in Fiji/ImageJ 1.48p.

For flowering time analysis, genotypes were grown in parallel under the indicated conditions and rosette leaf number before bolting was analyzed for at least 15 plants per genotype.

Yeast Two-Hybrid Interaction Studies

For interaction studies of PWO1 with CLF, SWN, and MEA, the vectors pGAD-PWO1-CDS, pGBD-PWO1-CDS, and pGAD-SWNΔSET were generated. Additional vectors used were pBD-CLFΔSET (Chanvivattana et al., 2004) and pAD-MEA-CDS (Lindner et al., 2013).

To generate pGAD-PWO1-CDS and pGBD-PWO1-CDS, a full-length cDNA was ordered (Riken RAFL16-55-O22) and used as template for PCR amplification of the complete PWO1 coding sequence (forward, ATGGCAAGTCCAGGATCAGGTGC; reverse, TTGAACTCTTCTTCTCTCGTTAAAGGC), which was cloned into the pCR8/GW/TOPO entry vector and subsequently recombined into the vectors pGBKT7-DEST and pGADT7-DEST (Horák et al., 2008).

All yeast techniques were performed as described in the Yeast Protocols Handbook (Clontech Laboratories; protocol PT3024-1, version PR13103). The yeast strains YST1 and AH109 were transformed with Gal4-BD and Gal4-AD constructs, respectively. After mating, yeast two-hybrid studies were performed by dilution series on selective media.

Gene Expression Analyses

Detection of GUS activity was performed as described previously (Colon-Carmona et al., 1999). Pools of 10-d-old, LD-grown seedlings were used for total RNA extraction (RNeasy Plant Mini Kit; Qiagen). RNA was resuspended in 50 μL RNase-free water, treated with DNase (Fermentas), transcribed into cDNA using SuperScriptIII following the manufacturer's instructions (Invitrogen), and subjected to real-time PCR. qRT-PCR analysis was performed with technical triplicates and three biological replicates (grown and harvested independently) using the oligonucleotides listed in Supplemental Table 2. The Mesa Blue Sybr Mix (Eurogentec) was used for amplification in a Chromo4 real-time PCR cycler (Bio-Rad). Expression levels were normalized to the reference gene At4g34270 (nblack) (Czechowski et al., 2005).

Coimmunoprecipitation Assays

Two-week-old Col-0, *PWO1$_{pro}$:PWO1-GFP*, and *PWO1$_{pro}$:PWO1-GFP 35S$_{pro}$:CLF-mCherry* seedlings were harvested and nuclear proteins were extracted from samples (4 g) as described (Smaczniak et al., 2012). To immunoprecipitate GFP fused proteins, nuclear proteins were incubated for 2 h at 4°C with 50 μL of μMACS anti-GFP MicroBeads (Miltenyi Biotec). Beads were immobilized in calibrated μcolumns (Miltenyi Biotec), washed six times with 200 μL of lysis buffer and two times with 200 μL of Wash Buffer 2; finally, bound proteins were eluted from the μcolumns with Elution Buffer preheated at 95°C (μMACS GFP Isolation Kit; Miltenyi Biotec). Eluted proteins were run on a 10% SDS-PAGE gel and transferred to PVDF membranes. Membranes were incubated with anti-DsRed antibody and anti-rabbit IgG coupled to HRP as primary and secondary antibodies, respectively. SuperSignal West Femto Chemiluminescent Substrate (Thermo Scientific) was used to develop the membranes and the signal was analyzed in a Fuji ImageQuant LAS4000. Details of antibodies used are listed in Supplemental Table 3.

PWO1-CDS and *PWO1$_{W63A}$-CDS* constructs were cloned in the pGEX-4T-3 vector (GE Healthcare) modified to be used with the Gateway system (Invitrogen). The plasmids were expressed in the *Escherichia coli* BL21 strain and proteins were purified using Glutathione-Sepharose 4B (Sigma-Aldrich; GE17-0756-01). Anti-H3 antibodies (Millipore; 05-928) were coupled to Dynabeads Protein A (Life Technologies; 10001D) and subsequently incubated with 5 to 7 ng of PWO1-GST or PWO1$_{W63A}$-GST proteins in 1× PBS for 4 h at 4°C. After incubation, the beads were washed three times with 1× PBS and resuspended in 2× SDS-PAGE loading buffer. Proteins were loaded in 10% SDS-PAGE gels and transferred to a PVDF membrane. Membranes were developed with anti-GST (Sigma-Aldrich; G7781) and anti-H3 (Diagenode; C15200011) antibodies.

Transient Colocalization Assay

Modified versions of pMDC7 carrying the GFP (pABindGFP) or mCherry (pABindCherry) coding sequence (Bleckmann et al., 2010) were used to insert the complete coding sequence of *PWO1* as well as truncations of *PWO1*, *CLF*, and *SWN* via Gateway cloning (Invitrogen).

Vectors were transformed in Agrobacterium GV3101 pMP90 carrying the silencing suppressor p19. For transient expression assays, the abaxial sides of leaves of 4-week-old *Nicotiana benthamiana* plants were infiltrated with Agrobacterium suspension as described (Bleckmann et al., 2010). Expression was induced by brushing 20 mM β-estradiol in 0.1% Tween onto infiltrated leaves 48 to 72 h after Agrobacterium infiltration,. To limit overexpression artifacts, fluorescence was monitored in leaf epidermis cells after a short induction period (4–6 h when fluorescence was visible) using a Zeiss LSM 710 confocal laser scanning microscope. Induction times for testing localization of different PWO1 variants were kept similar (fluorescence monitoring after 5 h of induction).

Chromatin Immunoprecipitation

Chromatin immunoprecipitations from 2 g of 2-week-old Col-0, *pwo1-1*, and *pwo1-1/3-2* pools of 10-d-old, LD-grown seedlings were performed using a Plant ChIP Kit (Diagenode; C01010150), following instructions given in the kit's protocol. Chromatin was sheared using a sonicator (Bioruptor Pico B01060001; Diagenode). For immunoprecipitations, anti-H3K27me3- and anti-H3-specific antibodies were employed (Supplemental Table 3). Three biological replicates were grown and harvested independently.

qPCR analyses were performed using SYBR Green I Master mix (Roche; 04887352001) and an iQ5 cycler detection system (Bio-Rad; 170-9780) using a two-step program. Ct values from input and immunoprecipitated samples were obtained in three technical replicates. Differences between genotypes were scored by comparison of percentage of input and SE values. Sequences of oligonucleotides used for ChIP analyses are listed in Supplemental Table 2.

Immunofluorescence

Roots of 10-d-old seedlings grown on GM medium were harvested and fixed in 4% PFA and nuclei were isolated essentially as described (Lysak et al., 2006). PWO1-GFP nuclear distribution was analyzed using immunofluorescence with anti-GFP antibodies and secondary antibodies as depicted in Supplemental Table 3 according to Lysak et al. (2006). DAPI staining of the nuclei was performed as described (Lysak et al., 2006).

Precipitation of GST Fusion Proteins with Biotinylated Peptides

Protein domains were expressed as GST fusion proteins (backbone pGEX4T3) in *E. coli* strains (Rosetta DE3). GST fusion protein expression was induced with 0.5 mM IPTG for 3 h at 28°C. Proteins were purified using the MagneGST pull-down system (Promega) according to the manufacturer's instructions. Purified GST fusion proteins were used for precipitation experiments with the biotinylated histone peptides listed in Supplemental Table 3 as described (Shi et al., 2006) with modifications: 1 μg of fusion protein was incubated with 1 μg of biotinylated peptide in 300 μL Gozani buffer (50 mM Tris-HCl, pH 7.5, 300 mM NaCl, 0.1% Igepal, 1 mM PEFA, and 1:100 plant protease inhibitor cocktail [Sigma-Aldrich; P9599]) overnight at 4°C on a rotating platform. Per sample, 15 μL of Streptavidin magnetic beads (Invitrogen) was added and the samples were incubated for 1 h at 4°C on a rotating platform. Beads were washed three times with 500 μL Gozani buffer at 4°C and then the bound proteins were eluted with 50 μL 0.1% SDS and incubated at 95°C for 5 min. The eluted proteins were studied by immunoblot analysis.

Modified Histone Peptide Array

The purified GST-PWO1-PWWP fusion protein was hybridized to a Modified Histone Peptide Array (Active Motif) to reveal binding specificity to modified histone peptides. The hybridization and analysis were performed as described (Bock et al., 2011).

Antibodies and Peptides

Antibodies and peptides used in this study are listed in Supplemental Table 3.

Accession Numbers

Sequence data from this article can be found in GenBank/EMBL data libraries under accession numbers At3g03140 (PWO1), At1g51745 (PWO2), At3g21295 (PWO3), At5g10140 (FLC), At2g23380 (CLF), At4g02020 (SWN), At1g02580 (MEA), At5g17690 (TFL2/LHP1), At1g24260 (SEP3), At4g18960 (AG), and At1g65480 (FT).

Supplemental Data

Supplemental Figure 1. Alignment of PWO1, PWO2, and PWO3 proteins.

Supplemental Figure 2. *PWO1*, *PWO2*, and *PWO3* gene structures, mutant alleles, and phenotypes of single and double mutants and complemented lines.

Supplemental Figure 3. Analysis of genetic interaction of *pwo1* and *clf* in SD conditions.

Supplemental Figure 4. Analysis of *FT* expression.

Supplemental Figure 5. H3 and H3K27me3 analyses in *pwo* mutants.

Supplemental Figure 6. Alignment of PWWP domains of Arabidopsis, mouse, human, and *S. pombe* proteins.

Supplemental Figure 7. PWO1-GFP signal intensity is not affected by the mutation of its PWWP domain.

Supplemental Table 1. Oligonucleotides for genotyping.

Supplemental Table 2. Oligonucleotides for RT-PCR and ChIP-PCR.

Supplemental Table 3. Antibodies and peptides used in this study.

ACKNOWLEDGMENTS

We gratefully acknowledge funding to support this research by the Deutsche Forschungsgemeinschaft through Grant SFB973 and the Boehringer Ingelheim Foundation and the European Commission Seventh Framework Programme People-2012-ITN Project EpiTRAITS (epigenetic regulation of economically important plant traits, number 316965). We thank Justin Goodrich for support for the initial yeast two-hybrid screen, Nora Lorberg for excellent technical assistance, José Luis Riechmann for providing the yeast two-hybrid cDNA library, Andrea Bleckmann for the modified pMDC7 vectors, the Nottingham Arabidopsis Stock Centre for seeds, and ABRC for DNA stocks. We also thank Celine Sabatel and Jean-Jacques Goval of Diagenode for their support and attention to protocol development for low chromatin amounts. We thank Justin Goodrich and members of the Schubert lab for critical reading of the manuscript.

AUTHOR CONTRIBUTIONS

M.L.H., P.M., S.F., and D.S. designed the research. M.L.H., S.F., P.M., O.K., C.K., and I.K. performed the experiments. I.K. and A.J. provided reagents. M.L.H., S.F., and D.S. wrote the article.

Received February 10, 2017; revised November 28, 2017; accepted January 9, 2018; published January 12, 2018.

REFERENCES

Alonso, J.M., et al. (2003). Genome-wide insertional mutagenesis of *Arabidopsis thaliana*. Science **301:** 653–657.

Alvarez-Venegas, R., and Avramova, Z. (2012). Evolution of the PWWP-domain encoding genes in the plant and animal lineages. BMC Evol. Biol. **12:** 101.

Ariel, F., Jegu, T., Latrasse, D., Romero-Barrios, N., Christ, A., Benhamed, M., and Crespi, M. (2014). Noncoding transcription by alternative RNA polymerases dynamically regulates an auxin-driven chromatin loop. Mol. Cell **55:** 383–396.

Bantignies, F., Roure, V., Comet, I., Leblanc, B., Schuettengruber, B., Bonnet, J., Tixier, V., Mas, A., and Cavalli, G. (2011). Polycomb-dependent regulatory contacts between distant Hox loci in Drosophila. Cell **144:** 214–226.

Barrero, J.M., González-Bayón, R., del Pozo, J.C., Ponce, M.R., and Micol, J.L. (2007). INCURVATA2 encodes the catalytic subunit of DNA Polymerase alpha and interacts with genes involved in chromatin-mediated cellular memory in *Arabidopsis thaliana*. Plant Cell **19:** 2822–2838.

Berger, N., Dubreucq, B., Roudier, F., Dubos, C., and Lepiniec, L. (2011). Transcriptional regulation of Arabidopsis LEAFY COTYLEDON2 involves RLE, a cis-element that regulates trimethylation of histone H3 at lysine-27. Plant Cell **23:** 4065–4078.

Bleckmann, A., Weidtkamp-Peters, S., Seidel, C.A., and Simon, R. (2010). Stem cell signaling in Arabidopsis requires CRN to localize CLV2 to the plasma membrane. Plant Physiol. **152:** 166–176.

Bock, I., Kudithipudi, S., Tamas, R., Kungulovski, G., Dhayalan, A., and Jeltsch, A. (2011). Application of Celluspots peptide arrays for the analysis of the binding specificity of epigenetic reading domains to modified histone tails. BMC Biochem. **12:** 48.

Bouyer, D., Roudier, F., Heese, M., Andersen, E.D., Gey, D., Nowack, M.K., Goodrich, J., Renou, J.P., Grini, P.E., Colot, V., and Schnittger, A. (2011). Polycomb repressive complex 2 controls the embryo-to-seedling phase transition. PLoS Genet. **7:** e1002014.

Butenko, Y., and Ohad, N. (2011). Polycomb-group mediated epigenetic mechanisms through plant evolution. Biochim. Biophys. Acta **1809:** 395–406.

Cai, L., et al. (2013). An H3K36 methylation-engaging Tudor motif of polycomb-like proteins mediates PRC2 complex targeting. Mol. Cell **49:** 571–582.

Calonje, M. (2014). PRC1 marks the difference in plant PcG repression. Mol. Plant **7:** 459–471.

Calonje, M., Sanchez, R., Chen, L., and Sung, Z.R. (2008). EMBRYONIC FLOWER1 participates in polycomb group-mediated AG gene silencing in Arabidopsis. Plant Cell **20:** 277–291.

Cao, R., Wang, L., Wang, H., Xia, L., Erdjument-Bromage, H., Tempst, P., Jones, R.S., and Zhang, Y. (2002). Role of histone H3 lysine 27 methylation in Polycomb-group silencing. Science **298:** 1039–1043.

Cao, R., Wang, H., He, J., Erdjument-Bromage, H., Tempst, P., and Zhang, Y. (2008). Role of hPHF1 in H3K27 methylation and Hox gene silencing. Mol. Cell. Biol. **28:** 1862–1872.

Cao, R., and Zhang, Y. (2004). The functions of E(Z)/EZH2-mediated methylation of lysine 27 in histone H3. Curr. Opin. Genet. Dev. **14:** 155–164.

Chanvivattana, Y., Bishopp, A., Schubert, D., Stock, C., Moon, Y.H., Sung, Z.R., and Goodrich, J. (2004). Interaction of Polycomb-group proteins controlling flowering in Arabidopsis. Development **131:** 5263–5276.

Clough, S.J., and Bent, A.F. (1998). Floral dip: a simplified method for Agrobacterium-mediated transformation of *Arabidopsis thaliana*. Plant J. **16:** 735–743.

Colon-Carmona, A., You, R., Haimovitch-Gal, T., and Doerner, P. (1999). Technical advance: spatio-temporal analysis of mitotic activity with a labile cyclin-GUS fusion protein. Plant J. **20:** 503–508.

Curtis, M.D., and Grossniklaus, U. (2003). A Gateway cloning vector set for high-throughput functional analysis of genes in planta. Plant Physiol. **133:** 462–469.

Czechowski, T., Stitt, M., Altmann, T., Udvardi, M.K., and Scheible, W.R. (2005). Genome-wide identification and testing of superior reference genes for transcript normalization in Arabidopsis. Plant Physiol. **139:** 5–17.

Czermin, B., Melfi, R., McCabe, D., Seitz, V., Imhof, A., and Pirrotta, V. (2002). Drosophila enhancer of Zeste/ESC complexes have a histone H3 methyltransferase activity that marks chromosomal Polycomb sites. Cell **111:** 185–196.

Del Prete, S., Mikulski, P., Schubert, D., and Gaudin, V. (2015). One, two, three: Polycomb proteins hit all dimensions of gene regulation. Genes (Basel) **6:** 520–542.

de Napoles, M., Mermoud, J.E., Wakao, R., Tang, Y.A., Endoh, M., Appanah, R., Nesterova, T.B., Silva, J., Otte, A.P., Vidal, M., Koseki, H., and Brockdorff, N. (2004). Polycomb group proteins Ring1A/B link ubiquitylation of histone H2A to heritable gene silencing and X inactivation. Dev. Cell **7:** 663–676.

Deng, W., Buzas, D.M., Ying, H., Robertson, M., Taylor, J., Peacock, W.J., Dennis, E.S., and Helliwell, C. (2013). Arabidopsis Polycomb Repressive Complex 2 binding sites contain putative GAGA factor binding motifs within coding regions of genes. BMC Genomics **14:** 593.

Derkacheva, M., Steinbach, Y., Wildhaber, T., Mozgová, I., Mahrez, W., Nanni, P., Bischof, S., Gruissem, W., and Hennig, L. (2013). Arabidopsis MSI1 connects LHP1 to PRC2 complexes. EMBO J. **32:** 2073–2085.

Dhayalan, A., Rajavelu, A., Rathert, P., Tamas, R., Jurkowska, R.Z., Ragozin, S., and Jeltsch, A. (2010). The Dnmt3a PWWP domain reads histone 3 lysine 36 trimethylation and guides DNA methylation. J. Biol. Chem. **285:** 26114–26120.

Farrona, S., Thorpe, F.L., Engelhorn, J., Adrian, J., Dong, X., Sarid-Krebs, L., Goodrich, J., and Turck, F. (2011). Tissue-specific expression of FLOWERING LOCUS T in Arabidopsis is maintained independently of polycomb group protein repression. Plant Cell **23:** 3204–3214.

Fischle, W., Wang, Y., Jacobs, S.A., Kim, Y., Allis, C.D., and Khorasanizadeh, S. (2003). Molecular basis for the discrimination of repressive methyl-lysine marks in histone H3 by Polycomb and HP1 chromodomains. Genes Dev. **17:** 1870–1881.

Förderer, A., Zhou, Y., and Turck, F. (2016). The age of multiplexity: recruitment and interactions of Polycomb complexes in plants. Curr. Opin. Plant Biol. **29:** 169–178.

Francis, N.J., Kingston, R.E., and Woodcock, C.L. (2004). Chromatin compaction by a polycomb group protein complex. Science **306:** 1574–1577.

Francis, N.J., Saurin, A.J., Shao, Z., and Kingston, R.E. (2001). Reconstitution of a functional core polycomb repressive complex. Mol. Cell **8:** 545–556.

Gaudin, V., Libault, M., Pouteau, S., Juul, T., Zhao, G., Lefebvre, D., and Grandjean, O. (2001). Mutations in LIKE HETEROCHROMATIN PROTEIN 1 affect flowering time and plant architecture in Arabidopsis. Development **128:** 4847–4858.

Gehani, S.S., Agrawal-Singh, S., Dietrich, N., Christophersen, N.S., Helin, K., and Hansen, K. (2010). Polycomb group protein displacement and gene activation through MSK-dependent H3K27me3S28 phosphorylation. Mol. Cell **39:** 886–900.

Gendall, A.R., Levy, Y.Y., Wilson, A., and Dean, C. (2001). The VERNALIZATION 2 gene mediates the epigenetic regulation of vernalization in Arabidopsis. Cell **107:** 525–535.

Gernand, D., Demidov, D., and Houben, A. (2003). The temporal and spatial pattern of histone H3 phosphorylation at serine 28 and serine 10 is similar in plants but differs between mono- and polycentric chromosomes. Cytogenet. Genome Res. **101:** 172–176.

Gong, W., Zhou, T., Mo, J., Perrett, S., Wang, J., and Feng, Y. (2012). Structural insight into recognition of methylated histone tails by retinoblastoma-binding protein 1. J. Biol. Chem. **287:** 8531–8540.

Goodrich, J., Puangsomlee, P., Martin, M., Long, D., Meyerowitz, E.M., and Coupland, G. (1997). A Polycomb-group gene regulates homeotic gene expression in Arabidopsis. Nature **386:** 44–51.

Goto, H., Tomono, Y., Ajiro, K., Kosako, H., Fujita, M., Sakurai, M., Okawa, K., Iwamatsu, A., Okigaki, T., Takahashi, T., and Inagaki, M.

(1999). Identification of a novel phosphorylation site on histone H3 coupled with mitotic chromosome condensation. J. Biol. Chem. **274:** 25543–25549.

Greb, T., Mylne, J.S., Crevillen, P., Geraldo, N., An, H., Gendall, A.R., and Dean, C. (2007). The PHD finger protein VRN5 functions in the epigenetic silencing of Arabidopsis FLC. Curr. Biol. **17:** 73–78.

Grossniklaus, U., Vielle-Calzada, J.P., Hoeppner, M.A., and Gagliano, W.B. (1998). Maternal control of embryogenesis by MEDEA, a polycomb group gene in Arabidopsis. Science **280:** 446–450.

Hecker, A., Brand, L.H., Peter, S., Simoncello, N., Kilian, J., Harter, K., Gaudin, V., and Wanke, D. (2015). The Arabidopsis GAGA-binding factor BASIC PENTACYSTEINE6 recruits the POLYCOMB-REPRESSIVE COMPLEX1 component LIKE HETEROCHROMATIN PROTEIN1 to GAGA DNA motifs. Plant Physiol. **168:** 1013–1024.

Heo, J.B., and Sung, S. (2011). Vernalization-mediated epigenetic silencing by a long intronic noncoding RNA. Science **331:** 76–79.

Hernández-Muñoz, I., Taghavi, P., Kuijl, C., Neefjes, J., and van Lohuizen, L.M. (2005). Association of BMI1 with polycomb bodies is dynamic and requires PRC2/EZH2 and the maintenance DNA methyltransferase DNMT1. Mol. Cell Biol. **25:** 11047–11058.

Horák, J., Grefen, C., Berendzen, K.W., Hahn, A., Stierhof, Y.D., Stadelhofer, B., Stahl, M., Koncz, C., and Harter, K. (2008). The Arabidopsis thaliana response regulator ARR22 is a putative AHP phospho-histidine phosphatase expressed in the chalaza of developing seeds. BMC Plant Biol. **8:** 77.

Illingworth, R.S., Moffat, M., Mann, A.R., Read, D., Hunter, C.J., Pradeepa, M.M., Adams, I.R., and Bickmore, W.A. (2015). The E3 ubiquitin ligase activity of RING1B is not essential for early mouse development. Genes Dev. **29:** 1897–1902.

Isono, K., Endo, T.A., Ku, M., Yamada, D., Suzuki, R., Sharif, J., Ishikura, T., Toyoda, T., Bernstein, B.E., and Koseki, H. (2013). SAM domain polymerization links subnuclear clustering of PRC1 to gene silencing. Dev. Cell **26:** 565–577.

Jiang, D., Wang, Y., Wang, Y., and He, Y. (2008). Repression of FLOWERING LOCUS C and FLOWERING LOCUS T by the Arabidopsis Polycomb repressive complex 2 components. PLoS One **3:** e3404.

Klose, R.J., Cooper, S., Farcas, A.M., Blackledge, N.P., and Brockdorff, N. (2013). Chromatin sampling–an emerging perspective on targeting polycomb repressor proteins. PLoS Genet. **9:** e1003717.

Köhler, C., Hennig, L., Bouveret, R., Gheyselinck, J., Grossniklaus, U., and Gruissem, W. (2003). Arabidopsis MSI1 is a component of the MEA/FIE Polycomb group complex and required for seed development. EMBO J. **22:** 4804–4814.

Kondo, T., Ito, S., and Koseki, H. (2016). Polycomb in transcriptional phase transition of developmental genes. Trends Biochem. Sci. **41:** 9–19.

Kuzmichev, A., Nishioka, K., Erdjument-Bromage, H., Tempst, P., and Reinberg, D. (2002). Histone methyltransferase activity associated with a human multiprotein complex containing the Enhancer of Zeste protein. Genes Dev. **16:** 2893–2905.

Kwiatkowska, D. (2004). Surface growth at the reproductive shoot apex of *Arabidopsis thaliana* pin-formed 1 and wild type. J. Exp. Bot. **55:** 1021–1032.

Lafos, M., Kroll, P., Hohenstatt, M.L., Thorpe, F.L., Clarenz, O., and Schubert, D. (2011). Dynamic regulation of H3K27 trimethylation during Arabidopsis differentiation. PLoS Genet. **7:** e1002040.

Larsson, A.S., Landberg, K., and Meeks-Wagner, D.R. (1998). The TERMINAL FLOWER2 (TFL2) gene controls the reproductive transition and meristem identity in *Arabidopsis thaliana*. Genetics **149:** 597–605.

Lau, P.N., and Cheung, P. (2011). Histone code pathway involving H3 S28 phosphorylation and K27 acetylation activates transcription and antagonizes polycomb silencing. Proc. Natl. Acad. Sci. USA **108:** 2801–2806.

Li, G., Zhang, J., Li, J., Yang, Z., Huang, H., and Xu, L. (2012). Imitation Switch chromatin remodeling factors and their interacting RINGLET proteins act together in controlling the plant vegetative phase in Arabidopsis. Plant J. **72:** 261–270.

Liang, S.C., et al. (2015). Kicking against the PRCs: A domesticated transposase antagonises silencing mediated by Polycomb group proteins and is an accessory component of Polycomb Repressive Complex 2. PLoS Genet. **11:** e1005660. Erratum. PLoS Genet. **12:** e1005812.

Libault, M., Tessadori, F., Germann, S., Snijder, B., Fransz, P., and Gaudin, V. (2005). The Arabidopsis LHP1 protein is a component of euchromatin. Planta **222:** 910–925.

Lindner, M., Simonini, S., Kooiker, M., Gagliardini, V., Somssich, M., Hohenstatt, M., Simon, R., Grossniklaus, U., and Kater, M.M. (2013). TAF13 interacts with PRC2 members and is essential for Arabidopsis seed development. Dev. Biol. **379:** 28–37.

Lodha, M., Marco, C.F., and Timmermans, M.C. (2013). The ASYMMETRIC LEAVES complex maintains repression of KNOX homeobox genes via direct recruitment of Polycomb-repressive complex2. Genes Dev. **27:** 596–601.

Lopez-Vernaza, M., Yang, S., Müller, R., Thorpe, F., de Leau, E., and Goodrich, J. (2012). Antagonistic roles of SEPALLATA3, FT and FLC genes as targets of the polycomb group gene CURLY LEAF. PLoS One **7:** e30715.

Luo, M., Bilodeau, P., Koltunow, A., Dennis, E.S., Peacock, W.J., and Chaudhury, A.M. (1999). Genes controlling fertilization-independent seed development in *Arabidopsis thaliana*. Proc. Natl. Acad. Sci. USA **96:** 296–301.

Lysak, M., Fransz, P., and Schubert, I. (2006). Cytogenetic analyses of Arabidopsis. Methods Mol. Biol. **323:** 173–186.

Maltby, V.E., Martin, B.J., Schulze, J.M., Johnson, I., Hentrich, T., Sharma, A., Kobor, M.S., and Howe, L. (2012). Histone H3 lysine 36 methylation targets the Isw1b remodeling complex to chromatin. Mol. Cell. Biol. **32:** 3479–3485.

Maurer-Stroh, S., Dickens, N.J., Hughes-Davies, L., Kouzarides, T., Eisenhaber, F., and Ponting, C.P. (2003). The Tudor domain 'Royal Family': Tudor, plant Agenet, Chromo, PWWP and MBT domains. Trends Biochem. Sci. **28:** 69–74.

Merini, W., and Calonje, M. (2015). PRC1 is taking the lead in PcG repression. Plant J. **83:** 110–120.

Michaels, S.D., and Amasino, R.M. (1999). FLOWERING LOCUS C encodes a novel MADS domain protein that acts as a repressor of flowering. Plant Cell **11:** 949–956.

Molitor, A.M., Bu, Z., Yu, Y., and Shen, W.H. (2014). Arabidopsis AL PHD-PRC1 complexes promote seed germination through H3K4me3-to-H3K27me3 chromatin state switch in repression of seed developmental genes. PLoS Genet. **10:** e1004091.

Mozgova, I., and Hennig, L. (2015). The polycomb group protein regulatory network. Annu. Rev. Plant Biol. **66:** 269–296.

Mozgova, I., Köhler, C., and Hennig, L. (2015). Keeping the gate closed: functions of the polycomb repressive complex PRC2 in development. Plant J. **83:** 121–132.

Müller, J., Hart, C.M., Francis, N.J., Vargas, M.L., Sengupta, A., Wild, B., Miller, E.L., O'Connor, M.B., Kingston, R.E., and Simon, J.A. (2002). Histone methyltransferase activity of a Drosophila Polycomb group repressor complex. Cell **111:** 197–208.

Nekrasov, M., Klymenko, T., Fraterman, S., Papp, B., Oktaba, K., Köcher, T., Cohen, A., Stunnenberg, H.G., Wilm, M., and Müller, J. (2007). Pcl-PRC2 is needed to generate high levels of H3-K27 trimethylation at Polycomb target genes. EMBO J. **26:** 4078–4088.

Oh, S., Park, S., and van Nocker, S. (2008). Genic and global functions for Paf1C in chromatin modification and gene expression in Arabidopsis. PLoS Genet. **4:** e1000077.

Ohad, N., Yadegari, R., Margossian, L., Hannon, M., Michaeli, D., Harada, J.J., Goldberg, R.B., and Fischer, R.L. (1999). Mutations in FIE, a WD polycomb group gene, allow endosperm development without fertilization. Plant Cell **11:** 407–416.

Ooi, S.K., Qiu, C., Bernstein, E., Li, K., Jia, D., Yang, Z., Erdjument-Bromage, H., Tempst, P., Lin, S.P., Allis, C.D., Cheng, X., and Bestor, T.H. (2007). DNMT3L connects unmethylated lysine 4 of histone H3 to de novo methylation of DNA. Nature **448:** 714–717.

Pazhouhandeh, M., Molinier, J., Berr, A., and Genschik, P. (2011). MSI4/FVE interacts with CUL4-DDB1 and a PRC2-like complex to control epigenetic regulation of flowering time in Arabidopsis. Proc. Natl. Acad. Sci. USA **108:** 3430–3435.

Pengelly, A.R., Kalb, R., Finkl, K., and Müller, J. (2015). Transcriptional repression by PRC1 in the absence of H2A monoubiquitylation. Genes Dev. **29:** 1487–1492.

Pirrotta, V., and Li, H.B. (2012). A view of nuclear Polycomb bodies. Curr. Opin. Genet. Dev. **22:** 101–109.

Qin, S., and Min, J. (2014). Structure and function of the nucleosome-binding PWWP domain. Trends Biochem. Sci. **39:** 536–547.

Qiu, C., Sawada, K., Zhang, X., and Cheng, X. (2002). The PWWP domain of mammalian DNA methyltransferase Dnmt3b defines a new family of DNA-binding folds. Nat. Struct. Biol. **9:** 217–224.

Roudier, F., et al. (2011). Integrative epigenomic mapping defines four main chromatin states in Arabidopsis. EMBO J. **30:** 1928–1938.

Sarma, K., Margueron, R., Ivanov, A., Pirrotta, V., and Reinberg, D. (2008). Ezh2 requires PHF1 to efficiently catalyze H3 lysine 27 trimethylation in vivo. Mol. Cell. Biol. **28:** 2718–2731.

Schatlowski, N., Stahl, Y., Hohenstatt, M.L., Goodrich, J., and Schubert, D. (2010). The CURLY LEAF interacting protein BLISTER controls expression of polycomb-group target genes and cellular differentiation of *Arabidopsis thaliana*. Plant Cell **22:** 2291–2305.

Schuettengruber, B., and Cavalli, G. (2009). Recruitment of polycomb group complexes and their role in the dynamic regulation of cell fate choice. Development **136:** 3531–3542.

Schuettengruber, B., Chourrout, D., Vervoort, M., Leblanc, B., and Cavalli, G. (2007). Genome regulation by polycomb and trithorax proteins. Cell **128:** 735–745.

Schwartz, Y.B., and Pirrotta, V. (2014). Ruled by ubiquitylation: a new order for polycomb recruitment. Cell Reports **8:** 321–325.

Sessions, A., et al. (2002). A high-throughput Arabidopsis reverse genetics system. Plant Cell **14:** 2985–2994.

Sewalt, R.G., van der Vlag, J., Gunster, M.J., Hamer, K.M., den Blaauwen, J.L., Satijn, D.P., Hendrix, T., van Driel, R., and Otte, A.P. (1998). Characterization of interactions between the mammalian polycomb-group proteins Enx1/EZH2 and EED suggests the existence of different mammalian polycomb-group protein complexes. Mol. Cell. Biol. **18:** 3586–3595.

Shao, Z., Raible, F., Mollaaghababa, R., Guyon, J.R., Wu, C.T., Bender, W., and Kingston, R.E. (1999). Stabilization of chromatin structure by PRC1, a Polycomb complex. Cell **98:** 37–46.

Sheldon, C.C., Burn, J.E., Perez, P.P., Metzger, J., Edwards, J.A., Peacock, W.J., and Dennis, E.S. (1999). The FLF MADS box gene: a repressor of flowering in Arabidopsis regulated by vernalization and methylation. Plant Cell **11:** 445–458.

Shi, X., et al. (2006). ING2 PHD domain links histone H3 lysine 4 methylation to active gene repression. Nature **442:** 96–99.

Simon, J.A., and Kingston, R.E. (2013). Occupying chromatin: Polycomb mechanisms for getting to genomic targets, stopping transcriptional traffic, and staying put. Mol. Cell **49:** 808–824.

Smaczniak, C., et al. (2012). Characterization of MADS-domain transcription factor complexes in Arabidopsis flower development. Proc. Natl. Acad. Sci. USA **109:** 1560–1565.

Sung, S., and Amasino, R.M. (2004). Vernalization in Arabidopsis thaliana is mediated by the PHD finger protein VIN3. Nature **427:** 159–164.

Till, B.J., et al. (2003). Large-scale discovery of induced point mutations with high-throughput TILLING. Genome Res. **13:** 524–530.

Turck, F., Roudier, F., Farrona, S., Martin-Magniette, M.L., Guillaume, E., Buisine, N., Gagnot, S., Martienssen, R.A., Coupland, G., and Colot, V. (2007). Arabidopsis TFL2/LHP1 specifically associates with genes marked by trimethylation of histone H3 lysine 27. PLoS Genet. **3:** e86.

Wang, H., Liu, C., Cheng, J., Liu, J., Zhang, L., He, C., Shen, W.H., Jin, H., Xu, L., and Zhang, Y. (2016). Arabidopsis flower and embryo developmental genes are repressed in seedlings by different combinations of Polycomb group proteins in association with distinct sets of cis-regulatory elements. PLoS Genet. **12:** e1005771.

Wang, H., Wang, L., Erdjument-Bromage, H., Vidal, M., Tempst, P., Jones, R.S., and Zhang, Y. (2004). Role of histone H2A ubiquitination in Polycomb silencing. Nature **431:** 873–878.

Wang, Y., Reddy, B., Thompson, J., Wang, H., Noma, K., Yates III, J.R., and Jia, S. (2009). Regulation of Set9-mediated H4K20 methylation by a PWWP domain protein. Mol. Cell **33:** 428–437.

Yoshida, N., Yanai, Y., Chen, L., Kato, Y., Hiratsuka, J., Miwa, T., Sung, Z.R., and Takahashi, S. (2001). EMBRYONIC FLOWER2, a novel polycomb group protein homolog, mediates shoot development and flowering in Arabidopsis. Plant Cell **13:** 2471–2481.

Xiao, J., et al. (2017). Cis and trans determinants of epigenetic silencing by Polycomb repressive complex 2 in Arabidopsis. Nat. Genet. **49:** 1546–1552.

Zemach, A., Li, Y., Ben-Meir, H., Oliva, M., Mosquna, A., Kiss, V., Avivi, Y., Ohad, N., and Grafi, G. (2006). Different domains control the localization and mobility of LIKE HETEROCHROMATIN PROTEIN1 in Arabidopsis nuclei. Plant Cell **18:** 133–145.

Zhang, X., Clarenz, O., Cokus, S., Bernatavichute, Y.V., Pellegrini, M., Goodrich, J., and Jacobsen, S.E. (2007). Whole-genome analysis of histone H3 lysine 27 trimethylation in Arabidopsis. PLoS Biol. **5:** e129.

Zhou, Y., Hartwig, B., James, G.V., Schneeberger, K., and Turck, F. (2016). Complementary activities of TELOMERE REPEAT BINDING proteins and Polycomb group complexes in transcriptional regulation of target genes. Plant Cell **28:** 87–101.

Zhou, Y., Tergemina, E., Cui, H., Förderer, A., Hartwig, B., Velikkakam James, G., Schneeberger, K., and Turck, F. (2017). Ctf4-related protein recruits LHP1-PRC2 to maintain H3K27me3 levels in dividing cells in *Arabidopsis thaliana*. Proc. Natl. Acad. Sci. USA **114:** 4833–4838.